SLOW LIGHT IN GERMANIUM NANOCRYSTALS

A THESIS

SUBMITTED TO THE DEPARTMENT OF PHYSICS

AND THE INSTITUTE OF ENGINEERING AND SCIENCE

OF BILKENT UNIVERSITY

IN PARTIAL FULFILLMENT OF THE REQUIREMENTS

FOR THE DEGREE OF

MASTER OF SCIENCE

By

Ümit Keleş

August, 2009

I certify that I have read this thesis and that in my opinion it is fully adequate, in scope and in quality, as a thesis for the degree of Master of Science.

_____
Assoc. Prof. Dr. Ceyhun Bulutay (Advisor)

I certify that I have read this thesis and that in my opinion it is fully adequate, in scope and in quality, as a thesis for the degree of Master of Science.

_____
Assoc. Prof. Dr. M. Özgür Oktel

I certify that I have read this thesis and that in my opinion it is fully adequate, in scope and in quality, as a thesis for the degree of Master of Science.

_____
Assoc. Prof. Dr. Bayram Tekin

Approved for the Institute of Engineering and Science:

_____
Prof. Dr. Mehmet B. Baray
Director of the Institute Engineering and Science

ABSTRACT

SLOW LIGHT IN GERMANIUM NANOCRYSTALS

Ümit Keleş

M.S. in Physics

Advisor: Assoc. Prof. Dr. Ceyhun Bulutay

August, 2009

The phenomena of quantum coherence has been applied with great success in the atomic systems. For optoelectronic applications the interest is inherently directed towards the semiconductor heterostructures. Large number of works have proposed and analyzed the atomic quantum coherence effects in the semiconductors. In this respect, nanocrystals (NCs) are very promising structures for seeking the quantum coherence phenomena due to their atomic-like electronic structure. Furthermore, their robust structure, integrability and larger excitonic lifetimes with respect to atomic systems makes them more promising candidates for the technological applications.

Within an atomistic pseudopotential electronic structure framework, the optical Bloch equations (OBEs) originating from atomic coherence theory are derived and solved numerically for Ge NCs. The results are interpreted in the context of coherent population oscillations (CPO). Narrow dips are observed in the absorption profiles which corresponds to high dispersions within a transparency window and produce slow light. A systematic study of the size-scaling of slow-down factor with respect to NC diameter and controllable slow light by applying external Stark field are provided. The results indicate that Ge NCs can be used to generate optically and electrically controllable slow light.

The many-body Coulomb interactions which underlie the quantum coherence and dephasing are of central importance in semiconductor quantum confined systems. The effects of many-body interactions on the optical response of Ge NCs have been analyzed. The semiconductor optical Bloch equations (SBEs) are derived in a semiclassical approach and the Coulomb correlations are included at the level of Hartree-Fock approximation.

ÖZET

GERMANYUM NANOÖRGÜLERDE YAVAŞ IŞIK

Ümit Keleş
Fizik, Yüksek Lisans
Tez Yöneticisi: Doç. Dr. Ceyhun Bulutay
Ağustos, 2009

Kuantum uyumluluğu temelli olgular atomik sistemlerde başarıyla uygulanmıştır. Teknolojik uygulamalar için ilgi yarıiletken malzemelere de kaydırılmıştır. Yarıiletkenlerde atomik kuantum uyumluluğu benzeri etkileri araştıran pek çok çalışma yapılmıştır. Bu bağlamda, nanoörgüler (NÖ'ler) atomik benzeri elektronik yapıları ile kuantum uyumluluğu etkilerinin gözlemlenmesi için gelecek vadeden malzemelerdir. Ayrıca, atomik sistemlere kıyasla istikrarlı yapıları, bütünleşebilirlik ve daha uzun uyarılmış kalabilme süreleri, bu malzemeleri teknolojik uygulamalar için daha uygun hale getirmektedir.

Uyguladığımız atomik görünür potansiyel temelli elektronik yapı hesabı dahilinde, atomik uyumluluk kuramına dayanan optik Bloch denklemleri türetilmiş ve germanyum (Ge) NÖ'leri için sayısal yöntemlerle çözülmüştür. Sonuçlar, uyumlu yoğunluk salınımları olgusu kapsamında değerlendirilmiştir. Soğurma görüngesindeki dar çukurluklar aynı bölgede yüksek dağılımlı geçirgenlik oluşturarak yavaş ışık gözlemlenmesini sağlamıştır. Yavaşlama oranının, NÖ çapına ve uygulanan dış Stark elektrik alanına bağlılığı incelenmiştir. Sonuçlarımız, Ge NÖ'lerinde optik ve elektriksel olarak kontrol edilebilecek yavaş ışık oluşturulabileceğini göstermiştir.

Kuantum uyumluluğunun ve uyarılmış durum sönümlülüğünün alt yapısını oluşturan çok parçacık Coulomb etkileşimleri, kuantum sınırlandırılmış sistemlerde ana öneme sahiptir. Çok parçacık etkileşimlerinin Ge NÖ'lerin optik tepkileri üzerindeki etkisi araştırılmıştır. Bu amaçla yarıiletken Bloch denklemleri türetilmiş ve Coulomb etkileri Hatree-Fock yaklaşımı kapsamında dahil edilmiştir.

Anahtar sözcükler: Nanoörgüleri, Yoğunluk Dizey Çözümlemesi, Optik Bloch Denklemleri, Yavaş Işık, İkinci Nicemleme, Yarıiletken Bloch Denklemleri.

Acknowledgement

I would like to express my gratitude to my advisor Assoc. Prof. Dr. Ceyhun Bulutay for his contributions to this thesis and my life.

Contents

List of Figures

List of Tables

Chapter 1

Introduction

Nanocrystals (NCs) are nanometer-scale semiconductor crystals where the carriers are spatially confined in all three dimensions. The quantum confinement effects breaks up the continuous density of states within the conduction and valence bands into discrete quantized states and leads to the discrete energy levels with sharp optical absorption spectra; similar to those of atoms and molecules. By these similarities, NCs are usually regarded as *artificial solid-state atoms* [1, 2, 3].

These similarities triggered numerous works to investigate the atomic-like properties in NCs. As expected atomic-like emission and absorption spectra of NCs observed in the early 1990s [4, 5, 6]. However, besides the atomic-like electronic and optical properties, NCs have several application advantages over the atomic systems. Since NCs are mesoscopic systems consisting of 10^3 to 10^6 individual atoms and molecules, there is a possibility of engineering the composition, size and shape of NCs. As such, one can control the energy levels and optical properties of NCs. The robust structure of NCs at room temperature is also a significant advantage over the atomic systems which can be captured only for the short durations via complicated cooling and trapping techniques [1]. Moreover, crystalline effects such as carrier-carrier and carrier-phonon interactions bring new properties to NCs which are not available in atomic systems. These advantages can be employed for technological applications, provided that we understand the fundamental physics of the electronic and optical properties

associated with NCs.

In this thesis, we follow the trail of some fundamental atomic quantum co-
herence effects on germanium (Ge) NCs. Besides their fundamental interest the
quantum coherence phenomena are important for the applications such as the
quantum computation [1] and slow light [7]. Our emphasis here is on the gener-
ation of slow light in Ge NCs.

Ge NCs embedded in silica exhibit atomic-like states which are very conve-
nient for the coherent control schemes. However, a more fundamental reason
for our consideration of Ge NCs is due to their lowest unoccupied molecular or-
bital (LUMO) level widely separated from the higher-lying states by more than
$250\ meV$ for NCs smaller than $2\ nm$; this property is unique and it is not the case
for instance for silicon NCs [8]. Hence, this advantageous electronic structure of
Ge NCs offers an ideal setting for exploring the quantum optical effects.
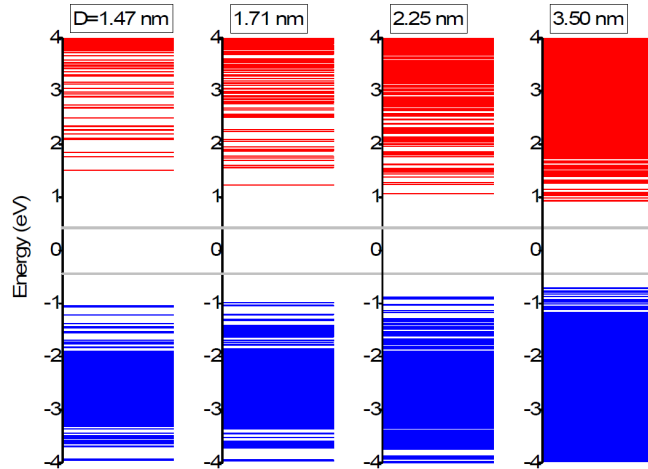
Figure 1.1: Energy spectra of germanium NCs of four different diameters em-
bedded in a wide bandgap matrix computed with our atomistic pseudopotential
approach; band edges of the bulk Ge is also marked as a reference [8].

In this computational expedition, aiming for a realistic account, the electronic
structure and optical dipole matrix elements are computed using an atomistic
pseudopotential approach; this is particularly challenging for a system containing

about several thousand atoms [9]. Figure 1.1 shows the evolution of the electronic states as the size of the Ge NCs varies; the widely-separated LUMO level for small diameters can be observed [8].

The velocity at which an optical pulse propagates through a material is given by the group velocity and expressed as,

$$\nu_g = \frac{c}{n + \omega \frac{dn}{d\omega}} \tag{1.1}$$

where c is the group velocity of the light in vacuum, ω is the angular velocity of the pulse and n is the refractive index of the material [7]. As Eq. (1.1) indicates the group velocity depends not only on the refractive index, but also on the refractive index dispersion (i.e. $\frac{dn}{d\omega}$). Usually the dispersion is so small then the group velocity is equal to $\frac{c}{n}$. Nevertheless, the group velocity can be reduced to very small limits by exploiting the refractive index dispersion value.

Slow light is important both for fundamental understanding of quantum coherence effects and promising for new applications in quantum information and information processing such as all-optical networks, controllable optical data buffers, and optical data storage and memories. However, for such applications main aim is not just slowing the light but more essentially generating a tunable time delay by controlling the group velocity. The capacity of an optical buffer in an optoelectronic devise is directly proportional to the variability of the group velocity [10].

When an electromagnetic field is slowed down in a medium, its energy density increases. Since the nonlinear effects depend on the local energy density, the spatial compression of optical energy can be used to enhance the nonlinear optical effects. By this way, the nonlinear effects can be observed at much more lower applied powers than usually required [11].

The key to produce slow light is to give a mechanism which can lead to a transparency window in the absorption spectra. However, although, the medium is highly transparent, there is still a strong dispersion to produce slow light. Any mechanism that burns a hole in the absorption and gives rapid spectral variation of refractive index can produce slow light [12].

In 1992, Harris *et al*. [13] estimated that the electromagnetically induced transparency (EIT) can be used to generate slow light. EIT is a quantum interference effect fundamentally based on the coherent population trapping in a three level system. Experimental observation of this mechanism to slow the light was reported by Hau *et al*. [14]. They reported a group velocity of about 17 m/s in a Bose-Einstein condensate. Using EIT many groups observed slow light in different material systems [15, 16, 17].

For possible applications interest is eventually directed towards the room temperature solid materials. The problem with EIT in those systems is large dephasing rates compared with gases that broaden spectral features and preclude strong dispersion required for the production of slow light.

Bigelow *et al*. [18] suggested a new mechanism, the coherent population oscillation (CPO) to produce slow light in a solid state material at room temperature. Unlike EIT, this new mechanism relies on a two-level system for the propagation material. They observed a group velocity of about 57 m/s in a ruby crystal at room temperature. Following their work, several other groups applied CPO mechanism to produce tunable slow light in semiconductor quantum wells and dots [19, 20, 32, 22].

CPO can be observed when a strong pump field and weak probe field with slightly different frequencies interact within a saturable absorber material. In this process the ground state population is induced to oscillate at the beat frequency between the pump and probe fields. When the beat frequency is smaller than or approximately equal to the inverse population relaxation time T_1^{-1}, the oscillation can lead to a sharp decrease of the absorption of the probe field and so a rapid frequency variation of the refractive index experienced by the probe field. Since such a rapid variation means $\frac{dn}{d\omega} > 0$, by Eq. (1.1), gives rise to small group velocities for the probe field.

The advantage of CPO over EIT is the former required long population relaxation times whereas the latter requires long dephasing times. In solid materials carrier-carrier and carrier-phonon scatterings give rise to very small dephasing times. Hence CPO is more adequate to implement slow light in the solid state

mediums. Actually we are going to see that short dephasing times are very crucial to generate the population oscillations.

In this Thesis, we use CPO to generate a transparency window within the absorption profile.

An analysis based on the atomic quantum theories does not give a complete description of semiconductor behavior, since the many-body interactions between the carriers are neglected. For a more realistic calculation the semiconductor effects should be included in a consistent manner. The inclusion of the many body effects into the atomic quantum coherence theory can be accomplished using the semiconductor Bloch equations [23]. The choice of nanocrystals becomes more meaningful in this sense since with their atomic-like properties NCs are best structures for the transition from atomic systems to semiconductors.

Due to the carrier-carrier scatterings, the redistribution of populations and the renormalization of energy levels are expected. Such contributions will modify the spectral shape and magnitude of quantum coherence effects [24]. When the many-body interactions are included to the calculations, the dephasing processes become significantly faster due to carrier-carrier and carrier-phonon collisions. Hence in order to maintain the coherence effects, higher coupling fields are required.

The main result of Coulomb interaction is the carrier-carrier scattering. If the external driving fields do not vary much in the typical carrier-carrier scattering time of less then picoseconds, the scatterings just drives the electron and hole distributions within each band to Fermi-Dirac distributions. Hence, carrier-carrier interactions can be included to the calculations by the effective rate approximations which describe in which rate the population distributions converge to the quasi-Fermi-Dirac distributions [25].

1.1   This Work

The organization of this Thesis is as follows:

In the following chapter we introduce the density matrix formalism of light-matter interaction and derive the optical Bloch equations for a multi-level system. The dephasing processes are included phenomenologically in terms of the relaxation and dephasing times. Next, we discuss the two-level approximation and present the analytical and numerical solution methods for the two-level OBEs.

In Chapter 3, we briefly describe our electronic structure calculations called linear combination of bulk bands (LCBB). Next, we illustrate that dephasing and relaxation times are very crucial inputs for the solutions of OBEs and thus we discuss the range of these values for Ge NCs. While solving OBEs for Ge NCs, we explain the hole burning phenomena and represent our results for slow light production in Ge NCs. We give the size-scaling of slow-down factor with respect to NC diameter and Stark effect.

In Chapter 4, we develop an analysis which explains the semiconductor quantum coherence phenomena in Ge nanocrystals. Due to the strong many-body effects, some deviations from the results of atomic coherence theory are inevitable. In that part, we treat the light-matter interaction in terms of second quantized electron-hole formulation. The semiconductor Bloch equations are introduced to investigate quantum coherence phenomena in semiconductors. The carrier-carrier and carrier-phonon interactions are included in the context of Hartree-Fock approximation. The collision effects beyond that approximation are added in terms of effective relaxation rates.

Chapter 5 contains the conclusion which gives aa brief discussion of all the preceding chapters and results of SBEs are expected as a future work.

Chapter 2

Optical Bloch Equations

In the present chapter we derive the density matrix formulation of the light-matter interaction. We consider the interaction for a multi-level system. After deriving the general formalism, we are going to concentrate on the physics of two-level scheme. A two-level approximation is useful when the two-levels of the interest to the medium are in resonance nearly with the applied fields whereas all the other levels are significantly detuned.

2.1   General Formalism

Quantum mechanically, one can specify the dynamic state of a single particle in terms of its state function. Similarly the dynamics of a quantum mechanical system can be specified in terms of a pure state function. On the other hand, in order to describe the state of a macroscopic medium containing many particles we need the complete knowledge of states of all the particles in the medium. In such a case we can apply the statistical mechanics in order to calculate the averaged expectation values of observable medium quantities. That is, we consider the probability distribution function $\mathcal{P}_i$ over all the possible states $|\psi_i\rangle$ of the system. Then the expectation value of some physical quantity represented by the operator

$\hat{\mathcal{O}}$ is averaged over the all possible states and given by

$$\langle \hat{\mathcal{O}} \rangle = \sum_i \mathcal{P}_i \langle \psi_i | \hat{\mathcal{O}} | \psi_i \rangle \,, \tag{2.1}$$

where $|\psi_i\rangle$ is a state of the complete set of orthonormal quantum states of many-particle system. The right hand side of Eq. (2.1) can be written in the matrix representation using an arbitrary complete basis set $|n\rangle$,

$$\langle \hat{\mathcal{O}} \rangle = \sum_{n,m} \sum_i \mathcal{P}_i \langle \psi_i | n \rangle \langle n | \hat{\mathcal{O}} | m \rangle \langle m | \psi_i \rangle \,. \tag{2.2}$$

Rearranging terms

$$\langle \hat{\mathcal{O}} \rangle = \sum_{n,m} \left[\sum_i \mathcal{P}_i \langle m | \psi_i \rangle \langle \psi_i | n \rangle \right] \langle n | \hat{\mathcal{O}} | m \rangle \,, \tag{2.3}$$

which can be written as

$$\langle \hat{\mathcal{O}} \rangle = \sum_{n,m} \langle m | \hat{\rho} | n \rangle \langle n | \hat{\mathcal{O}} | m \rangle \,, \tag{2.4}$$

where we defined the element of a matrix, called the density matrix

$$\rho_{mn} = \langle m | \hat{\rho} | n \rangle = \sum_i \mathcal{P}_i \langle m | \psi_i \rangle \langle \psi_i | n \rangle \,, \tag{2.5}$$

and the corresponding density operator is

$$\hat{\rho} \equiv \sum_i \mathcal{P}_i | \psi_i \rangle \langle \psi_i | \,. \tag{2.6}$$

Then Eq.(2.4) will be

$$\langle \hat{\mathcal{O}} \rangle = \sum_m \langle m | \hat{\rho} \hat{\mathcal{O}} | m \rangle = tr(\hat{\rho} \hat{\mathcal{O}}) \,, \tag{2.7}$$

where we used tr, trace that is the sum of the diagonal elements and invariant to any unitary transformation of the representation. Hence the expectation value is independent of any specific representation. Let us here make a remark that as long as our equations are linear, we can effectively replace the operators in equations by their expectation values, i.e., $\hat{\rho}_{nm} \rightarrow \langle \hat{\rho}_{nm} \rangle \equiv \rho_{nm}$. This can be performed by taking the expectation values of both sides of equations. Hence we drop the *hats* of operators, since their meanings can be understood from the content.

The elements of density matrix have significant physical interpretations. Consider for example, our multi-level system of light-matter interaction. The *diagonal matrix elements* are real by Eq. (2.5),

$$\rho_{nn} = \sum_i \mathcal{P}_i |\langle n|\psi_i\rangle|^2 \,, \tag{2.8}$$

where the probability, that a particle in the state $|\psi_i\rangle$ will be found in the level $|n\rangle$ is averaged over all the states occupied by the particles of the medium. Hence this value corresponds to the *population distribution* on the level $|n\rangle$.

On the other hand, the off-diagonal elements ρ_{nm} are the averages of the product of the expansion coefficients $\langle n|\psi_i\rangle$ and $\langle m|\psi_i\rangle$, and they have a complex conjugate property

$$\rho_{nm} = \sum_i \mathcal{P}_i \langle n|\psi_i\rangle\langle\psi_i|m\rangle = \sum_i \mathcal{P}_i^* \langle m|\psi_i\rangle^*\langle\psi_i|n\rangle^* = \rho_{mn}^* \,. \tag{2.9}$$

Since the expansion coefficients are complex in general, we can write them as amplitudes and phases

$$\rho_{nm} = \sum_i \mathcal{P}_i \left[|\langle n|\psi_i\rangle||\langle\psi_i|m\rangle|e^{i(\phi_n-\phi_m)} \right] \,. \tag{2.10}$$

If neither of the expansion coefficients is equal to zero, then whether the off-diagonal elements vanish or not will depend on whether the relative phase factor $(\phi_n - \phi_m)$ averages to zero or not. If the wave functions are incoherent with randomly distributed relative phases, then the off-diagonal elements average to zero. So the *off-diagonal element* ρ_{nm} is *a measure of the coherence* between the levels n and m, in the sense that it will be nonzero if the system is in a coherent superposition of energy eigenstates $|n\rangle$ and $|m\rangle$.

We can understand the significance of coherence considering the macroscopic electric polarization of a medium via induced dipole moment. The macroscopic polarization is given as

$$\vec{P} = N\langle\vec{\mu}\rangle \,, \tag{2.11}$$

in terms of the expectation value of dipole moment μ where N is the dipole number density of the medium. The dipole matrix elements are

$$\vec{\mu}_{nm} = \vec{\mu}_{mn}^* = -e\langle n|\hat{r}|m\rangle \,, \tag{2.12}$$

where $-e$ is the electron charge and $\hat{r}$ is the position operator for the electron. By the assumption that the wave functions corresponding to states $|n\rangle$ and $|m\rangle$ have definite parity, the diagonal elements $\langle n|\hat{r}|n\rangle$ vanish as a consequence of symmetry considerations. It also means that the medium has no permanent dipole. Consider for the sake of clarity the expectation value of dipole moment for a two-level system, $\langle\vec{\mu}\rangle = tr(\rho\vec{\mu})$ where $\rho\vec{\mu}$ is represented as

$$\langle\vec{\mu}\rangle = tr(\rho\vec{\mu}) = tr\left(\begin{bmatrix} \rho_{11} & \rho_{12} \\ \rho_{21} & \rho_{22} \end{bmatrix}\begin{bmatrix} 0 & \vec{\mu}_{12} \\ \vec{\mu}_{21} & 0 \end{bmatrix}\right) = tr\left(\begin{bmatrix} \rho_{12}\vec{\mu}_{21} & \rho_{11}\vec{\mu}_{12} \\ \rho_{22}\vec{\mu}_{21} & \rho_{21}\vec{\mu}_{12} \end{bmatrix}\right), \tag{2.13}$$

thus the expectation value of dipole moment is

$$\langle\vec{\mu}\rangle = tr(\rho\vec{\mu}) = \rho_{12}\vec{\mu}_{21} + \rho_{21}\vec{\mu}_{12}. \tag{2.14}$$

Hence, we observe that the expectation value of the dipole moment depends on the off-diagonal elements of the density matrix. That is, the off-diagonal elements are a measure of the macroscopic polarization of the medium. This illustrates the importance of off-diagonal elements since from the polarization we can switch to other macroscopic properties of the medium [24].

For future reference, combining Eqs. (2.11) and (2.14), we obtain the macroscopic polarization in terms of dipole moments and density matrices,

$$\vec{P}(t) = N\left[\rho_{12}(t)\vec{\mu}_{21} + \rho_{21}(t)\vec{\mu}_{12}\right], \tag{2.15}$$

where N is again the density of dipole moments. On the other hand, the linear polarization in the frequency domain is related to the complex susceptibility of the medium by

$$\vec{P}_i(\omega) = \epsilon_b\chi_{ij}(\omega)\vec{\mathcal{E}}_j(\omega) \tag{2.16}$$

where the subscripts i and j indicate the Cartesian components and ϵ_b is the host material dielectric constant [39]. In an anisotropic medium, χ is a tensor. However, in the homogeneously spherical NCs it turns out just a scalar quantity.

After a Fourier transformation, the macroscopic polarization given in Eq. (2.15) can also be written in the frequency domain. This gives rise to the relation [39],

$$\vec{P}(\omega) = \epsilon_b\tilde{\chi}(\omega)\vec{\mathcal{E}}(\omega) = N\left[\rho_{12}(\omega)\vec{\mu}_{21} + \rho_{21}(\omega)\vec{\mu}_{12}\right], \tag{2.17}$$

from which we can extract the susceptibility,

$$\tilde{\chi}(\omega) = \frac{N\left[\rho_{12}(\omega)\vec{\mu}_{21} + \rho_{21}(\omega)\vec{\mu}_{12}\right]}{\epsilon_b \vec{\mathcal{E}}(\omega)} \, . \tag{2.18}$$

The propagation of an electromagnetic field in a dispersive medium can be characterized by the frequency dependent complex susceptibility, $\chi = \chi' + i\chi''$. We assume small field amplitudes so that the medium displays only linear response. The imaginary part of the susceptibility, χ'' gives the absorption of the medium whereas the real part, χ' corresponds to the dispersion of the medium [27]. We will return to these discussions when we are ready to solve density matrices in the frequency domain.

Hence in summary, the diagonal elements of density matrix give the relative populations of energy levels and the off-diagonal elements, in our case, takes part in the calculation of polarization. The dynamics of the multi-level system, thus the evolution of populations and polarization over time can be described by the time dependence of the density matrix.

From the definition of ρ, we can observe that it can evolve in time by two reasons. One is the time dependence of the probability function $\mathcal{P}_i(t)$ of the state $|\psi_i\rangle$. Other is the time-dependence of the state function $|\psi_i\rangle$, itself. Thus we can write the time evolution of ρ by using its definition given by Eq. (2.6),

$$\frac{d}{dt}\rho = \sum_i \left[\left(\frac{\partial}{\partial t}|\psi_i(t)\rangle\right)\mathcal{P}_i\langle\psi_i| + |\psi_i\rangle\left(\frac{\partial}{\partial t}\mathcal{P}_i(t)\right)\langle\psi_i| + |\psi_i\rangle\mathcal{P}_i\left(\frac{\partial}{\partial t}\langle\psi_i(t)|\right) \right] \, . \tag{2.19}$$

Assume that our system has no relaxation process or no random forces, i.e., all the particles experience the the same forces. So all the particles in the medium can be described by the same Hamiltonian. That is in the absence of relaxation processes, the probability of each state conserved and the probability distribution function $\mathcal{P}_i$ does not change explicitly with time,

$$\frac{\partial}{\partial t}\mathcal{P}_i = 0 \, . \tag{2.20}$$

Since we stated that all the particles have the same Hamiltonian, then by the Schrödinger Equation

$$\frac{\partial}{\partial t}|\psi_i(t)\rangle = -\frac{i}{\hbar}\mathcal{H}|\psi_i(t)\rangle \quad \text{and} \quad \frac{\partial}{\partial t}\langle\psi_i(t)| = \frac{i}{\hbar}\langle\psi_i(t)|\mathcal{H} \, . \tag{2.21}$$

Inserting Eqs. (2.20) and (2.21) into (2.19) we obtain the equation of motion for $\hat{\rho}$ in the absence of relaxation processes,

$$\dot{\rho} = -\frac{i}{\hbar}\left[\mathcal{H}, \rho\right] . \tag{2.22}$$

This equation is known as the Liouville equation which describes the time evolution of density operator.

So far we excluded the relaxation processes which are always present in real media. The randomizing forces corresponding to the relaxation processes (such as collisions between particles) act differently on each particle. Since there is no way of calculating exactly these random forces, they may be approximated phenomenologically. We expect a general form of

$$\dot{\rho} = -\frac{i}{\hbar}\left[\mathcal{H}, \rho\right] + \left(\frac{\partial \rho}{\partial t}\right)_{rel} , \tag{2.23}$$

where the term $(\partial\rho/\partial t)_{rel}$ reflects the relaxation effects since our condition of Eq. (2.20) is not valid any more. The relaxation can be included to the formalism in several ways. Rigorously one can introduce the master equation which contains system-reservoir interactions, then solve the corresponding equations of motions [37, 38]. Nevertheless, the reasoning of that method indicates that the relaxation processes can be described quite well by adding phenomenological damping terms to the density matrix equation,

$$\dot{\rho}_{nm} = -\frac{i}{\hbar}\left[\mathcal{H}, \rho\right]_{nm} - \gamma_{nm}\left(\rho_{nm} - \rho_{nm}^{(eq)}\right) , \tag{2.24}$$

which means if the medium is not too far from thermal equilibrium, ρ_{nm} relaxes to its equilibrium value ρ_{nm} at rate γ_{nm}. When the system is in thermal equilibrium the excited states may contain population, i.e., $\rho_{nm}^{(eq)}$ can be nonzero. However, the thermal excitation is expected to be an incoherent process so that cannot produce any coherent superposition of states. Thus the off-diagonal elements average to zero, $\rho_{nm}^{(eq)} = 0$ for $n \neq m$. Since γ_{nm} is a decay rate, we can also write $\gamma_{nm} = \gamma_{mn}$.

Alternatively, in a different approach, for the diagonal elements we may allow population decays from higher levels to lower levels. Assuming above discussion

still describes the off-diagonal elements, we write the density matrix equations,

$$\dot{\rho}_{nm} = -\frac{i}{\hbar}\left[\mathcal{H}, \rho\right]_{nm} + \sum_{E_m > E_n} \Gamma_{nm}\rho_{mm} - \sum_{E_n > E_m} \Gamma_{mn}\rho_{nn}, \qquad (2.25)$$

where Γ_{nm} is the rate of population decay from level $|m\rangle$ to level $|n\rangle$, and Γ_{nm} is the damping rate of γ_{nm} coherence. The diagonal and off-diagonal damping rates are related in a way

$$\gamma_{nm} = \frac{1}{2}\left(\Gamma_n + \Gamma_m\right) + \gamma_{nm}^{(pro)}, \qquad (2.26)$$

where Γ_n and Γ_m are the total decay rates of population out of levels $|n\rangle$ and $|m\rangle$, respectively, i.e.,

$$\Gamma_n = \sum_{E_n > E_n'} \Gamma_{n'n}, \qquad (2.27)$$

and $\gamma_{nm}^{(pro)}$ is the proper dephasing rate which collects the dephasing processes that are not related with the population transfer such as collisions.

We can relate above relaxation rates with relaxation times which are more explicit for us. Following the first approach to the relaxation processes, in the language of quantum optics, the diagonal relaxation rates corresponds to population relaxation time of level $|n\rangle$, $\gamma_{nn}^{-1} = T_{nn}$. The off-diagonal relaxation rates correspond to polarization dephasing time, $\gamma_{nm}^{-1} = T_{nm}$. Its name originates from Eqs. (2.11-2.14) since dipole moment dephases in this characteristic time. In a two-level system T_{nn} and T_{nm} are usually denoted as T_1 and T_2 or for a multi-level system $(T_1)_{nn}$ and $(T_2)_{nm}$, respectively. T_1 and T_2 terminology originates from the magnetic resonance phenomena in which literature T_1-time is referred to as longitudinal relaxation time and T_2-time is referred to as transverse relaxation time [40].

Due to energetic considerations, it is always easier to change the phase rather than altering the populations in a relaxation process so that T_2 is always shorter than corresponding T_1. The difference in relaxation times, their values and their comparison with other system parameters give rise to important physical consequences as we are going to see in the following sections.

2.2 Multi-Level System

So far we introduced the general idea of density matrix equation. Now we can specify this equation for the light-matter interaction problems. Let us rewrite the density matrix equation of motion that we are supposed to solve,

$$\dot{\rho}_{nm} = -\frac{i}{\hbar} [\mathcal{H}, \rho]_{nm} - \frac{\rho_{nm} - \rho_{nm}^{(eq)}}{T_{nm}} . \tag{2.28}$$

First, consider the absence of external perturbation and relaxation processes. In such a case the density matrix equation gets the form

$$\dot{\rho}_{nm} = -\frac{i}{\hbar} [\mathcal{H}_o, \rho]_{nm} . \tag{2.29}$$

Since there is no perturbation, we can assume that the time-independent Schrodinger equation

$$\mathcal{H}_o |n\rangle = E_n |n\rangle , \tag{2.30}$$

can be solved. For our multi-level system this will give the interaction-free energies of levels, i.e., $E_n = \hbar\omega_n$. Thus we can write

$$\begin{aligned}
\dot{\rho}_{nm} &= -\frac{i}{\hbar} [\mathcal{H}_o, \rho]_{nm} = -\frac{i}{\hbar} (\mathcal{H}_o\rho - \rho\mathcal{H}_o)_{nm} = -\frac{i}{\hbar} \sum_j (\mathcal{H}_{o,nj}\rho_{jm} - \rho_{nj}\mathcal{H}_{o,jm}) \\
&= -\frac{i}{\hbar} \sum_j (E_n\delta_{nj}\rho_{jm} - \rho_{nj}\delta_{jm}E_m) = -\frac{i}{\hbar} (E_n\rho_{nm} - E_m\rho_{nm}) = -i\omega_{nm}\rho_{nm} ,
\end{aligned}$$

where we defined the transition frequency $\omega_{nm} \equiv (E_n - E_m)/\hbar$.

Next, if we subject the medium to a time-dependent external perturbation, the total Hamiltonian will be

$$\mathcal{H} = \mathcal{H}_o + \mathcal{V}(t) , \tag{2.31}$$

where the operator $\mathcal{V}(t)$ represents the perturbation and $\mathcal{H}_o$ is the unperturbed Hamiltonian. Then the density matrix equation is

$$\dot{\rho}_{nm} = -\frac{i}{\hbar} [\mathcal{H}, \rho]_{nm} = -\frac{i}{\hbar} [\mathcal{H}_o, \rho]_{nm} - \frac{i}{\hbar} [\mathcal{V}, \rho]_{nm} , \tag{2.32}$$

where we can write

$$[\mathcal{V}, \rho]_{nm} = (\mathcal{V}\rho - \rho\mathcal{V})_{nm} = \sum_j (\mathcal{V}_{nj}\rho_{jm} - \rho_{nj}\mathcal{V}_{jm}) . \tag{2.33}$$

For the interaction of electromagnetic radiation with an optical medium, we can specify the perturbation using the electric dipole approximation,

$$\mathcal{V}(t) = -\vec{\mu} \cdot \vec{\mathcal{E}}(t) \,, \tag{2.34}$$

where $\vec{\mu}$ is the electric dipole moment. In this approximation it is assumed that the wavelength of the electromagnetic field is much larger than the size of medium. So the amplitude of the field does not vary across the medium. This allows us to write $\vec{\mathcal{E}}(z,t) \to \vec{\mathcal{E}}(t)$. We also ignore the effects of magnetic field [41]. Following Eq. (2.12), the matrix representation of interaction potential is given as

$$\mathcal{V}_{nm} = \mathcal{V}_{mn}^* = -\vec{\mu}_{nm} \cdot \vec{\mathcal{E}}(t) \,. \tag{2.35}$$

For the electromagnetic field, we are going to use a pump-probe scheme. In pump-probe experiments, a strong pump field and a weak probe field excites the medium simultaneously [42]. The frequency of the probe field is going to be scanned around the frequency of the pump field. Working within the framework of semiclassical laser theory, we treat the applied fields classically and the medium quantum mechanically. So we write the total bichromatic field as

$$\vec{\mathcal{E}}(t) = \vec{\mathcal{E}}_s e^{-i\omega_s t} + \vec{\mathcal{E}}_p e^{-i\omega_p t} + \vec{\mathcal{E}}_s^* e^{i\omega_s t} + \vec{\mathcal{E}}_p^* e^{i\omega_p t} \,, \tag{2.36}$$

where $\mathcal{E}_i$ are complex amplitudes, ω_i is the frequency and the subscripts s and p identify the strong pump and weak probe fields.

Finally including the relaxation times we can write the general form of density matrix equation of motion for the optical medium coupling to electromagnetic fields,

$$\dot{\rho}_{nm} = -i\omega_{nm}\rho_{nm} - \frac{\rho_{nm} - \rho_{nm}^{(eq)}}{T_{nm}} + \frac{i}{\hbar} \sum_j \left(\vec{\mu}_{nj} \cdot \vec{\mathcal{E}}(t)\rho_{jm} - \rho_{nj}\vec{\mu}_{jm} \cdot \vec{\mathcal{E}}(t) \right) \,. \tag{2.37}$$

We can further specify n and m values, and solve the resulting density matrix equations. Let us consider the two-level model.
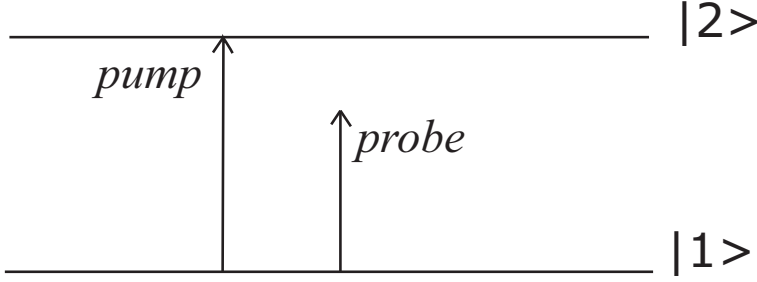
Figure 2.1: Two-level model

2.3 Two-Level System

We consider a two-level system. The lower level is denoted $|1\rangle$ and the upper level $|2\rangle$ as illustrated in Fig. 2.1. In Eq. (2.37) we run n and m values over 1 and 2 to obtain the density matrix equations of the system,

$$\dot{\rho}_{21} = -i\omega_{21}\rho_{21} - \frac{\rho_{21}}{(T_2)_{21}} + \frac{i}{\hbar}\left(\vec{\mu}_{21}\cdot\vec{\mathcal{E}}(t)\rho_{11} - \rho_{22}\vec{\mu}_{21}\cdot\vec{\mathcal{E}}(t)\right), \qquad (2.38)$$

$$\dot{\rho}_{11} = -\frac{\rho_{11} - \rho_{11}^{(eq)}}{(T_1)_{11}} + \frac{i}{\hbar}\left(\vec{\mu}_{12}\cdot\vec{\mathcal{E}}(t)\rho_{21} - \rho_{12}\vec{\mu}_{21}\cdot\vec{\mathcal{E}}(t)\right), \qquad (2.39)$$

$$\dot{\rho}_{22} = -\frac{\rho_{22} - \rho_{22}^{(eq)}}{(T_1)_{22}} + \frac{i}{\hbar}\left(\vec{\mu}_{21}\cdot\vec{\mathcal{E}}(t)\rho_{12} - \rho_{21}\vec{\mu}_{12}\cdot\vec{\mathcal{E}}(t)\right), \qquad (2.40)$$

where we used the results of previous part such that $\rho_{nm}^{(eq)} = 0$ for $n \neq m$ and $\mu_{nn} = 0$ by the parity of wave functions. Due to the relation $\rho_{12} = \rho_{21}^*$ that we showed in Eq. (2.9), no separate equation is required for ρ_{12}.

In a closed two-level system, the total population $\rho_{22} + \rho_{11}$ is conserved. This means that a decrease in one population should cause an increase in the other population, or vice versa. This gives rise to $\dot{\rho}_{22} + \dot{\rho}_{11} = 0$ and since $T_{nm} = T_{mn}$ we can write $(T_1)_{22} = (T_1)_{11} \equiv T_1$. By the same reason, for the coherence dephasing times we have $(T_2)_{21} = (T_2)_{12} \equiv T_2$.

Since Eq. (2.38) depends on the populations ρ_{22} and ρ_{11} by their difference $\rho_{22} - \rho_{11}$, it may be useful to write the equations of motions in terms of population

difference $\rho_{22} - \rho_{11}$. Subtracting Eq. (2.39) from Eq. (2.40) we obtain

$$\dot{\rho}_{22} - \dot{\rho}_{11} = -\frac{(\rho_{22} - \rho_{11}) - (\rho_{22} - \rho_{11})^{(eq)}}{T_1} + \frac{2i}{\hbar}\left(\vec{\mu}_{21} \cdot \vec{\mathcal{E}}(t)\rho_{12} - \rho_{21}\vec{\mu}_{12} \cdot \vec{\mathcal{E}}(t)\right).$$
(2.41)

For the electric field we use Eq. (2.36), thus we obtain the optical Bloch equations (OBEs) for a two-level system,

$$\dot{\rho}_{21} = -\left(i\omega_{21} + \frac{1}{T_2}\right)\rho_{21} - \frac{i}{\hbar}\overrightarrow{\mu}_{21} \cdot \left[\vec{\mathcal{E}}_s e^{-i\omega_s t} + \vec{\mathcal{E}}_p e^{-i\omega_p t} + \vec{\mathcal{E}}_s^* e^{i\omega_s t} + \vec{\mathcal{E}}_p^* e^{i\omega_p t}\right](\rho_{22} - \rho_{11}),$$
(2.42)

$$
\begin{aligned}
(\dot{\rho}_{22} - \dot{\rho}_{11}) &= -\frac{(\rho_{22} - \rho_{11}) - (\rho_{22} - \rho_{11})^{(eq)}}{T_1} \\
&+ \frac{2i}{\hbar}\vec{\mu}_{21} \cdot \left[\vec{\mathcal{E}}_s e^{-i\omega_s t} + \vec{\mathcal{E}}_p e^{-i\omega_p t} + \vec{\mathcal{E}}_s^* e^{i\omega_s t} + \vec{\mathcal{E}}_p^* e^{i\omega_p t}\right]\rho_{12} \\
&- \frac{2i}{\hbar}\vec{\mu}_{12} \cdot \left[\vec{\mathcal{E}}_s e^{-i\omega_s t} + \vec{\mathcal{E}}_p e^{-i\omega_p t} + \vec{\mathcal{E}}_s^* e^{i\omega_s t} + \vec{\mathcal{E}}_p^* e^{i\omega_p t}\right]\rho_{21}.
\end{aligned}
$$
(2.43)

Now we are supposed to solve these coupled equation in order to understand the response of the two-level system to the pump-probe fields. The usual way of solution is applying an analytic method which was extensively discussed in the classical paper [27] and also can be found in [26],[11] and [7]. We solved the density matrix equations numerically without their approximations. Their solutions are valid for the steady state with the approximation of treating the strong field $\mathcal{E}_s$ correctly to all orders while treating the weak field $\mathcal{E}_p$ to only first order. Under this assumption they observe by inspection that the solution of Eqs. (2.42-2.43) for $\rho_{22}(t) - \rho_{11}(t)$ will have the form,

$$\rho_{22}(t) - \rho_{11}(t) = (\rho_{22} - \rho_{11})^{(0)} + (\rho_{22} - \rho_{11})^{(\delta)}e^{-i\delta t} + (\rho_{22} - \rho_{11})^{(-\delta)}e^{i\delta t},$$
(2.44)

where $\delta \equiv \omega_s - \omega_p$ is the beat frequency. This equation illustrates that the population difference of two levels has components oscillating with the beat frequency. This oscillatory behavior of populations is called the coherent population oscillations (CPO). To observe the oscillations the population relaxation rate $\gamma_1 = 1/T_1$ should be larger compared with the beat frequency, δ.

In steady state solution [7, 11, 27] the transition element of density matrix ρ_{21} exhibits harmonic oscillations with frequency components at $n\omega_s + m\omega_p$, where n

and m are integers. With the above approximation that the probe field $\mathcal{E}_p$ is weak and treated only to first order whereas the pump field $\mathcal{E}_s$ is strong and treated to all orders, it is also observed by inspection of Eqs. (2.42-2.43) that the solution for $\rho_{21}(t)$ oscillates dominantly at three frequencies: ω_s, ω_p, and $2\omega_s - \omega_p$. Thus the steady state solution for $\rho_{21}(t)$ can be expressed as following Ref. [27],

$$\rho_{21}(t) = \rho_{21}(\omega_s)e^{-i\omega_s t} + \rho_{21}(\omega_p)e^{-i\omega_p t} + \rho_{21}(2\omega_s - \omega_p)e^{-i(2\omega_s - \omega_p)t}, \qquad (2.45)$$

where $\rho_{21}(\omega_i)$ are called Fourier amplitudes and defined as

$$\rho_{21}(\omega_s) = \frac{\Omega_s(\rho_{22} - \rho_{11})^{dc}}{2(\omega_s - \omega_{21} + i/T_2)}, \qquad (2.46)$$

$$\begin{aligned}
\rho_{21}(\omega_p) &= \frac{\Omega_p(\rho_{22} - \rho_{11})^{dc}}{2D(\omega_p)}\left[\left(\omega_p - \omega_s + \frac{i}{T_1}\right)\left(\omega_p - 2\omega_s + \omega_{21} + \frac{i}{T_2}\right)\right. \\
&\quad \left. - \frac{\Omega_s^2(\omega_p - \omega_s)}{2(\omega_s - \omega_{21} - i/T_2)}\right],
\end{aligned}$$

$$\rho_{21}(2\omega_s - \omega_p) = \frac{\Omega_s^2\Omega_p(\rho_{22} - \rho_{11})^{dc}(\omega_p - \omega_s + 2i/T_2)}{4D(\omega_p)(\omega_s - \omega_{21} - i/T_2)}, \qquad (2.47)$$

where $\Omega_i = 2|\mathcal{E}_i||\mu_{21}|/\hbar$ is the on-resonance Rabi frequency for the electric field of amplitude $2\mathcal{E}_i$ and $(\rho_{22} - \rho_{11})^{dc}$ the steady-state saturated population inversion induced by the pump field $\mathcal{E}_s$ is defined as

$$(\rho_{22} - \rho_{11})^{dc} = \frac{\left[1 + (\omega_s - \omega_{21})^2 T_2^2\right](\rho_{22} - \rho_{11})^0}{1 + (\omega_s - \omega_{21})^2 T_2^2 + \Omega_s^2 T_1 T_2}, \qquad (2.48)$$

and the so called cubic function, $D(\omega_p)$ is

$$D(\omega_p) = (\omega_p - \omega_s + i/T_1)(\omega_p - \omega_{21} + i/T_2)(\omega_p - 2\omega_s + \omega_{21} + i/T_2) - \Omega_s^2(\omega_p - \omega_s + i/T_2). \qquad (2.49)$$

The physical meanings of Fourier amplitudes are important. The final one $\rho_{21}(2\omega_s - \omega_p)$ gives rise to generation of a field with frequency $\omega = 2\omega_s - \omega_p$. If a wave with this frequency already exist in the medium than it may be amplified. Similarly $\rho_{21}(\omega_s)$ and $\rho_{21}(\omega_p)$ give rise to absorption or amplification of the pump and probe fields, respectively. For our purposes the amplitude $\rho_{21}(\omega_p)$ is the crucial term.

In the mathematical language, the density matrix Eqs. (2.42-2.43) are coupled first-order differential equations which can be solved numerically with several

different methods to obtain $\rho_{21}(t)$ and $\rho_{22}(t) - \rho_{11}(t)$ [28]. We preferred the fourth order Runge-Kutta method [28]. The relaxation times are on the orders of nanoseconds for Ge NCs. For such relaxation times, time steps on the order of 10 ps produce proper results. In order to obtain smooth absorption curves, we observe the system up to 50 μs time range.

Since we are mainly interested with $\rho_{21}(\omega_p)$, we should switch from $\rho_{21}(t)$ to $\rho_{21}(\omega)$. This can be done by Fourier transformation of ρ_{21} from time space to frequency space. We get the Fourier transform as

$$\rho_{21}(\omega) = \frac{1}{2\pi} \int_{-\infty}^{\infty} \rho_{21}(t)e^{i\omega t}dt \,. \tag{2.50}$$

Nonetheless, for our purposes we do not need the whole spectrum of ω for ρ_{21} since we are interested just in $\rho_{21}(\omega_p)$. Thus we can set $\omega = \omega_p$ in Eq. (2.50) to get

$$\rho_{21}(\omega_p) = \frac{1}{2\pi} \int_{-\infty}^{\infty} \rho_{21}(t)e^{i\omega_p t}dt \,. \tag{2.51}$$

This was the theoretical discussion of Fourier transformation, but computationally of course we can not run $(-\infty, +\infty)$ interval. Since the response starts at $t = 0$, we have $\rho_{21}(t < 0) = 0$. That brings the lower limit of integration from $-\infty$ to zero. For the upper limit, we should cut the integration at a sufficiently long time $t = T$. This is physically meaningful because our system of light-matter interaction converges to a steady state rapidly. Following the theory of Fourier transformation since our limits of integration changed from $(-\infty, +\infty)$ to $(0, T)$, we should also change the $1/2\pi$ coefficient of integration by $1/T$, thus finally we get

$$\rho_{21}(\omega_p) = \frac{1}{T} \int_{0}^{T} \rho_{21}(t)e^{i\omega_p t}dt \,. \tag{2.52}$$

Although, the OBEs given in Eqs. (2.42) and (2.43) can be solved while in those forms, the rapid oscillatory behavior of exponential parts increases the calculation time. In order to simplify the calculations, we see from Eq. (2.42) that the nondriven (i.e., $\mathcal{E}(t)$) behavior of ρ_{21} is $\rho_{21}(t) = \rho_{21}(0)e^{-(i\omega_{21}+1/T_2)t}$ so that, for $\omega_p \approx \omega_{21}$, it is useful to introduce some slowly varying variables σ_{21} and σ_{12} as

$$\rho_{21}(t) = \sigma_{21}(t)e^{-i\omega_p t}$$

$$\rho_{12}(t) \;\; = \;\; \rho_{21}^*(t) = \sigma_{12}(t)e^{i\omega_p t}\,, \tag{2.53}$$

inserting these new variables into OBEs, we get:

$$\dot{\sigma}_{21} = -\left[i(\omega_{21}-\omega_p)+\frac{1}{T_2}\right]\sigma_{21}-\frac{i}{\hbar}\vec{\mu}_{21}\cdot\left[\vec{\mathcal{E}}_s e^{-i(\omega_s-\omega_p)t}+\vec{\mathcal{E}}_p\right](\rho_{22}-\rho_{11})\,, \tag{2.54}$$

$$
\begin{aligned}
(\dot{\rho}_{22}-\dot{\rho}_{11}) = \;\; - \;\; & \frac{(\rho_{22}-\rho_{11})-(\rho_{22}-\rho_{11})^{(eq)}}{T_1}+\frac{2i}{\hbar}\vec{\mu}_{21}\cdot\left[\vec{\mathcal{E}}_s e^{-i(\omega_s-\omega_p)t}+\vec{\mathcal{E}}_p\right]\sigma_{12} \\
& -\frac{2i}{\hbar}\vec{\mu}_{12}\cdot\left[\vec{\mathcal{E}}_s^* e^{i(\omega_s-\omega_p)t}+\vec{\mathcal{E}}_p^*\right]\sigma_{21}\,, \tag{2.55}
\end{aligned}
$$

where we eliminated terms with time dependence $e^{\pm i(\omega_s+\omega_p)t}$ and $e^{\pm i2\omega_p t}$, since they oscillate rapidly and their contribution averages to zero in a short time compared to that of observation. This approximation is called the rotating wave approximation (RWA). Although, such an implementation lengthen the analytical derivations, it reduces the computation times on the order of more than 10^5.

Notice that by the definition of new operator σ, the transform given in Eq. (2.52) gets a simpler form,

$$\rho_{21}(\omega_p) = \frac{1}{T}\int_0^T \sigma_{21}(t)dt\,. \tag{2.56}$$

Above Eqs. (2.54) and (2.55) explicitly manifest that the dynamics of a optically excited system is determined by population relaxation time T_1 and dephasing time T_2. Since the population relaxation also implies the phase relaxation of the optically excited dipoles, T_1 should be related to T_2, the decay of interband polarization. In the absence of collisional decays, the population lifetime of excited state, T_1 is twice the coherence dephasing time, T_2, i.e.,

$$\frac{1}{T_2} = \frac{1}{2T_1}\,, \tag{2.57}$$

for a two-level system [2, 3]. So this relation holds in the case of pure dephasing due to the finite lifetime of excited state. In general, different phase destroying processes are involved in dephasing dynamics giving a sum over different times T_i,

$$\frac{1}{T_2} = \frac{1}{2T_1}+\sum_i\frac{1}{T_i}\,. \tag{2.58}$$

These phase destroying processes are the coupling to different types of phonons, phase destroying scattering between carriers in a interacting many-body system and scattering at defects or interfaces [2]. It is difficult to determine different process times but in any case Eq. (2.58) comprises the relation

$$\frac{T_2}{T_1} \leq 2\,, \tag{2.59}$$

which actually sets an upper limit for T_2 since population relaxation always leads to dephasing of coherence.

So far we obtained the optical Bloch equations for a two-level system. In the next chapter we implement our derivations to the Ge NCs.

Chapter 3

Slow Light in the Optical Bloch Equations Level

When we consider the OBEs, Eqs. (2.54) and (2.55) derived in the preceding chapter, we notice that the medium material is described in the equations via the energy levels, electric dipole moments, and relaxation and dephasing times. In this chapter, first of all we briefly introduce our electronic structure calculations. Then we discuss the relaxation and dephasing times for Ge NCs. Finally, we solve the OBEs for Ge NCs and interpret the results within the context of slow light.

3.1   Electronic Structure Calculations

For the electronic structure calculations of large-scale nanostructure systems Wang and Zunger developed the linear combinations of bulk bands (LCBB) method [44]. The method introduces an effective calculation for the single-particle electronic states of million-atom nanostructure systems. The approach is fundamentally based on an empirical pseudopotential Hamiltonian. After calculating the electronic structure for bulk constituent materials, the wave functions of the nanostructure is expanded in terms of bulk Bloch states of the constituent materials. The expansion is performed over the bulk band indices, n and wave vectors,

k defined within the first Brilloin zone of a computational supercell which is periodic in all three dimensions. This choise economizes the basis size compared to plane wave type of approaches.

The main advantage of LCBB is very small calculation time of electronic structure even for million-atom nanostructures. Note that *ab initio* calculations are still science fiction for atomic systems containing more than 1000 atoms.

The main ingredients of LCBB are the atomic positions and the atomic pseudopotentials. The method gives the atomistic level wave functions which let us calculate the Coulomb interaction explicitly. Our bulk electronic structure calculations are based on the empirical pseudopotential method (EPM) which is also very fast, accurate and easy to implement [45, 46]. Moreover, particularly unlike *ab initio* calculations, EPM agrees with the experimental bandgap very accurately by its construction.

While implementing the LCBB method, we expand the jth state NC wave function in terms of the linear combinations of bulk Bloch bands of the constituent core and embedding medium materials,

$$\psi_j(\vec{r}) = \frac{1}{\sqrt{N}} \sum_{n,\vec{k},\sigma} C^\sigma_{n,\vec{k},j} \, e^{i\vec{k}\cdot\vec{r}} u^\sigma_{n,\vec{k}}(\vec{r}) \,, \tag{3.1}$$

where N is the number of primitive cells in the supercell and the superscript σ indicates the core or embedding medium materials. $u^\sigma_{n,\vec{k}}(\vec{r})$ is the cell-periodic part of the Bloch states and can be expanded by the plane wave functions of reciprocal-lattice vectors $\{\vec{G}\}$ as

$$u^\sigma_{n,\vec{k}}(\vec{r}) = \frac{1}{\sqrt{V_0}} \sum_{\vec{G}} B^\sigma_{n\vec{k}}\left(\vec{G}\right) e^{i\vec{G}\cdot\vec{r}}, \tag{3.2}$$

where V_0 is the volume of the primitive cell.

Our demand is to determine the expansion coefficients $C^\sigma_{n,\vec{k},j}$ defined in Eq. (3.1). For that we start by writing the single-particle atomistic pseudopotential Hamiltonian of the system,

$$\hat{H} = -\frac{\hbar^2\nabla^2}{2m} + \sum_{\sigma,\vec{R}_j,\alpha} W^\sigma_\alpha(\vec{R}_j)\, v^\sigma_\alpha\left(\vec{r} - \vec{R}_j - \vec{d}^\sigma_\alpha\right) \,, \tag{3.3}$$

where m is the free electron mass, $\vec{R}_j$ is the position of the primitive cell and $\vec{d}_\alpha^\sigma$ gives the relative coordinate of atom of type (σ, α) within the primitive cell. The weight function $W_\alpha^\sigma(\vec{R}_j)$ takes values 0 or 1 depending on whether an atom of type α is located at the position $\vec{R}_j + \vec{d}_\alpha^\sigma$. The screened spherical atomic pseudopotential v_α^σ is determined by reproducing a large variety of empirical results such as bulk band structures, effective masses, and deformation potentials.

Then the coefficients $C_{n,\vec{k},j}^\sigma$ can be obtained by solving the following eigenvalue equation [44, 47]:

$$\sum_{n,\vec{k},\sigma} H_{n'\vec{k}'\sigma',n\vec{k}\sigma}\, C_{n,\vec{k}}^\sigma = E \sum_{n,\vec{k},\sigma} S_{n'\vec{k}'\sigma',n\vec{k}\sigma}\, C_{n,\vec{k}}^\sigma, \tag{3.4}$$

where

$$H_{n'\vec{k}'\sigma',n\vec{k}\sigma} \equiv \left\langle n'\vec{k}'\sigma' | \hat{T} + \hat{V}_{\mathrm{xtal}} | n\vec{k}\sigma \right\rangle,$$

$$\left\langle n'\vec{k}'\sigma' | \hat{T} | n\vec{k}\sigma \right\rangle = \delta_{\vec{k}',\vec{k}} \sum_{\vec{G}} \frac{\hbar^2}{2m} \left| \vec{G} + \vec{k} \right|^2 B_{n'\vec{k}'}^{\sigma'} \left(\vec{G} \right)^* B_{n\vec{k}}^{\sigma} \left(\vec{G} \right),$$

$$\begin{aligned} \left\langle n'\vec{k}'\sigma' | \hat{V}_{\mathrm{xtal}} | n\vec{k}\sigma \right\rangle &= \sum_{\vec{G},\vec{G}'} B_{n'\vec{k}'}^{\sigma'} \left(\vec{G} \right)^* B_{n\vec{k}}^{\sigma} \left(\vec{G} \right) \\ &\times \sum_{\sigma'',\alpha} V_\alpha^{\sigma''} \left(\left| \vec{G} + \vec{k} - \vec{G}' - \vec{k}' \right|^2 \right) \\ &\times W_\alpha^{\sigma''} \left(\vec{k} - \vec{k}' \right) e^{i \left(\vec{G} + \vec{k} - \vec{G}' - \vec{k}' \right) \cdot \vec{d}_\alpha^{\sigma''}}, \end{aligned}$$

$$S_{n'\vec{k}'\sigma',n\vec{k}\sigma} \equiv \left\langle n'\vec{k}'\sigma' | n\vec{k}\sigma \right\rangle.$$

while implementing this eigenvalue equation we assumed both the constituent core and embedding medium to have the same lattice constant. They are placed within a computational supercell which satisfies the periodicity condition $W(\vec{R}_{n_1,n_2,n_3} + N_i \vec{a}_i) = W(\vec{R}_{n_1,n_2,n_3})$.

In this work, the constituent core material is Ge whereas for the embedding medium instead of a free-standing NC, we used an artificial wide band-gap material which satisfies the Ge/SiO_2 band alignment. We set the lattice constant and crystal structure of the embedding material equal to the diamond Ge to overcome the actual strain effects.

Within this method, we obtained the electronic structure and wave functions for different size Ge NCs (recall Fig. 1.1). Using the wave functions and Eq. (2.12), we calculated the electric dipole matrix elements. These quantities are required in order to solve OBEs for Ge NCs. Besides the electronic structure (i.e., energy levels of states) and electric dipole matrix elements, dephasing and relaxation times specifies the OBEs for a specific material.

Before presenting our results, we should give further technical preliminaries. As we are going to see in the Results part, in some cases when the probe field gets close to pump field its absorption decreases. This sharp dip in the absorption curve is called as *hole burning.*

3.2 Hole Burning

Hole burning in homogeneously saturable absorbers is an interesting property. Indeed at the early times of hole burning, it was commonly believed that the hole burning was a property of just *inhomogeneous* broadening [29, 30]. Consider an inhomogeneous medium with different excitation energies. When a probe field is applied to this medium with varying frequency, the absorption of the field will be a classical Lorentzian lineshape which means that the field experiences higher absorption in the vicinity of resonant transitions. However, if a strong pump field is applied to this medium in addition to weak probe field, the pump field will saturate the population differences whose transition frequencies are nearly in resonance with the pump field (see Fig. 3.1). The transitions at highly detuned frequencies will be untouched. Now with increasing power of this pump field, a sharp hole appears in the absorption line of the probe field. This hole is *burned* by the pump field in the vicinity of its frequency. The absorption of the probe field sharply decreases at the frequencies close to that of the pump field since those transitions are already saturated due to Pauli blocking by the strong pump field [30, 31, 32].
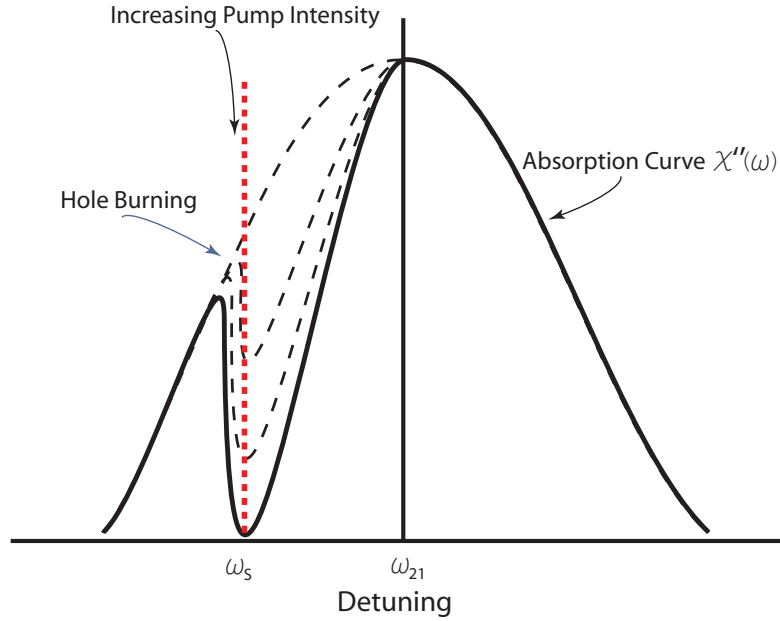
Figure 3.1: Saturation of absorption in an inhomogeneous transition.

On the other hand, it is commonly believed that for the homogeneous broad-ened transition, the increasing strength of pump field will further saturate the probe field absorption uniformly without changing its shape or linewidth and cannot have such a hole, see Fig. 3.2. However, the hole burning effect in a pump-probe experiment for a homogeneously broadened medium was first ob-served by Soffer and McFarland [33] in 1966 and explained by Schwarz and Tan [26] in 1967. They and many other authors [34, 35] attributed the origin of such a hole to the periodic modulation of the ground state population at the beat frequency $\delta = \omega_s - \omega_p$ between the pump and probe fields. As we mentioned in the previous section this phenomenon is called as coherent population oscillation (CPO). If the beat frequency between the fields is less than or approximately equal to the inverse of the population relaxation time T_1^{-1} then the population can follow the oscillations of optical intensity and the absorption of the probe field will decrease (see Fig. 3.3). We have T_1 here since it is the timescale within which the population oscillation can follow the beating induced by the fields.

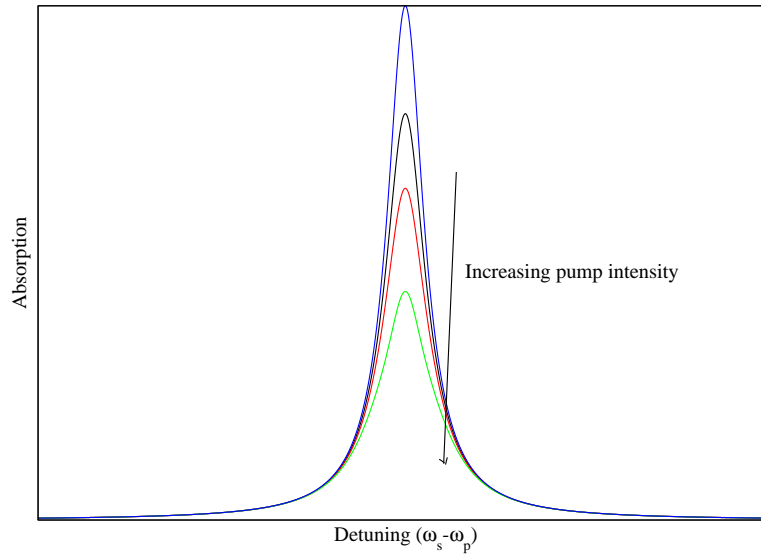Boyd and Mukamel [34] studied the theory of pump-probe experiment via

Figure 3.2: Saturation of absorption in a homogeneous transition.

the nonlinear susceptibility $\chi^{(3)}$. They showed that the general assumption of pump-probe experiments that the pump field prepares the system and then a nonsaturating weak probe field monitors the system is not accurate enough to calculate the probe field absorption. In the sequential treatment of the fields, one first calculates the steady state just under the effect of pump field and then calculates the response of perturbed system to the probe field [36]. However, they showed that the sequential treatment omits the interference terms between the two fields which give rise to the hole burning in the probe absorption profile. They calculated a contribution term to the usual absorption which results in a dip in the lineshape. Keeping this remark in mind, we solve the density matrix equations applying both fields simultaneously.

Although one can burn a hole on any region of the absorption spectrum (see Fig. 3.4), the deepest hole can be burned at the maximum of absorption spectrum. This means that the location of the spectral hole follows the frequency of pump field. Hence, the pump field does not need to be frequency locked to any specific transition. In order to get the maximum efficiency, we set the frequency of pump field in resonance with the difference between the HOMO-LUMO levels.
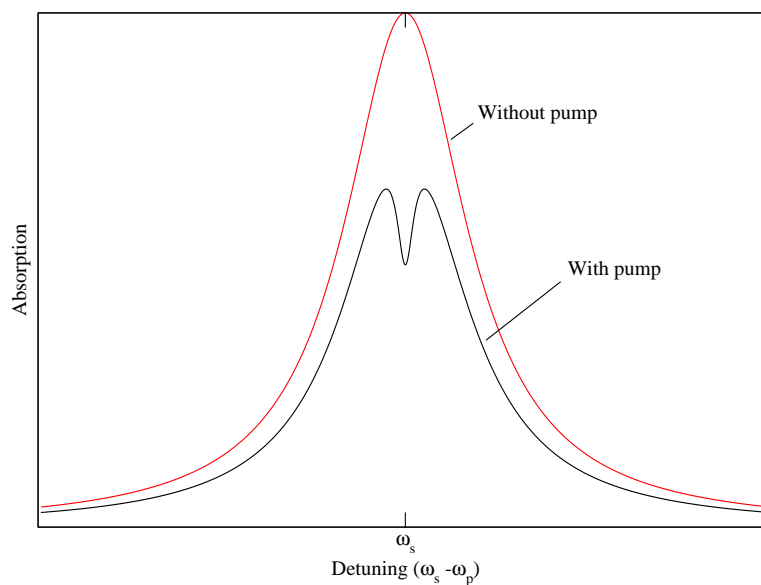
Figure 3.3: This population oscillation becomes significant when the detuning is smaller than the inverse of population lifetime and gives rise to an absorption dip on the absorption profile.
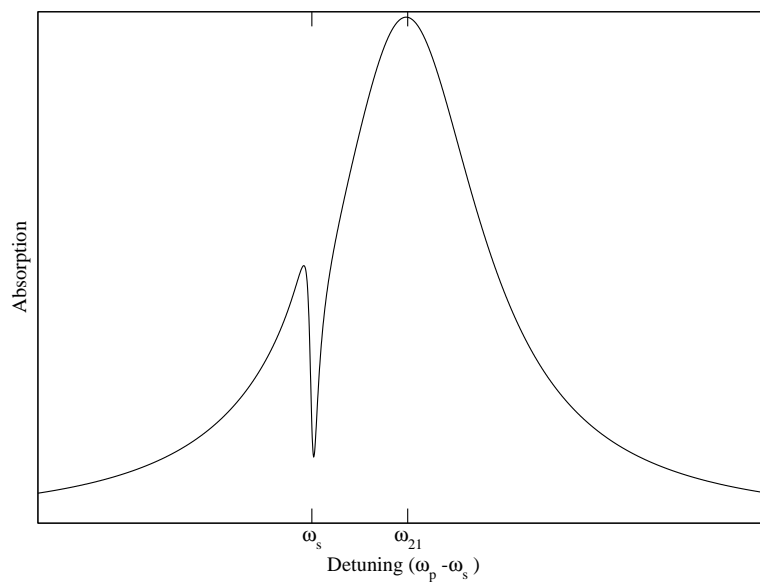

Figure 3.4: The hole burned at the wing of the absorption spectra.
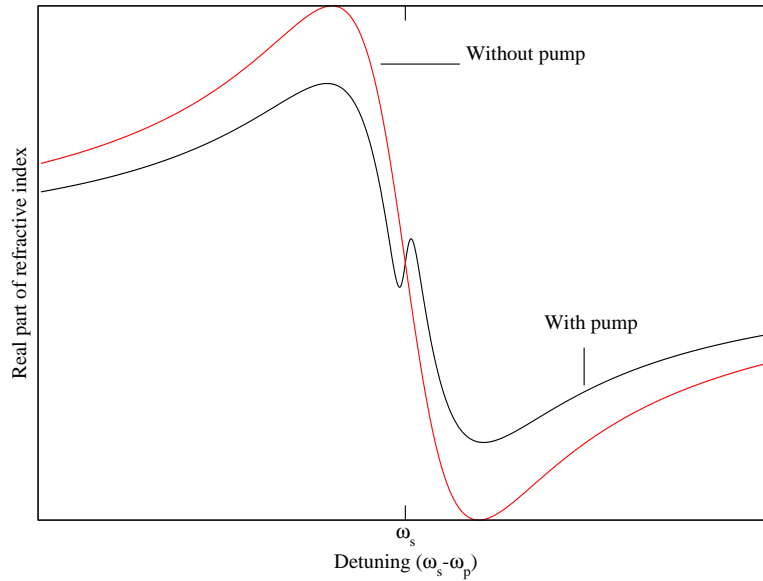
Figure 3.5: Variation of the refractive index by pump application.

A dip in the absorption spectrum has significant consequences such as saturation spectroscopy [30] and manipulation of the speed of light. Since the absorption hole has a width of $2T_1^{-1}$, this effect has been employed to measure the population lifetime in the saturation spectroscopy. The slow light is our next discussion.

3.3 Slow Light

The Kramer-Kronig relations, a consequence of causality condition, relate the absorption to the real part of the refractive index [7]. By this relation a narrow dip in the absorption spectrum will lead to a variation of the refractive index spectrum with a positive slope in the same frequency range, i.e., $\frac{\partial n}{\partial \omega} > 0$ (see Fig. 3.5). The induced population oscillation gives rise to a new polarization component thus alters the susceptibility and the refractive index experienced by the probe field.

The importance of this result can be understood, if we remember the definition

of group velocity also given in the Chapter 1,

$$v_g = \frac{d\omega}{dk} = \frac{c}{n + \omega\frac{\partial n}{\partial \omega}} \qquad (3.5)$$

where c is the speed of light in vacuum and n is the refractive index [7]. As we mentioned earlier, the large values of the refractive index dispersion can give rise to very small group velocities.

On the other hand, if we consider the opposite case, a narrow peak in the absorption spectrum corresponds to a large negative slope and produce superluminal ($v_g > c$) light propagation [7]. Despite the name superluminal, there is no contradiction with the second postulate of special relativity since no information can be sent faster than c, the speed of light in vacuum [48].

Following the definition of group velocity, we can also introduce the slowdown factor defined as

$$S = \frac{c}{v_g} = n + \omega\frac{\partial n}{\partial \omega}, \qquad (3.6)$$

which is indeed equal to the group index.

The refractive index is defined in terms of the dielectric function ϵ as,

$$n = \sqrt{\frac{\sqrt{Re\{\epsilon\}^2 + Im\{\epsilon\}^2} + Re\{\epsilon\}}{2}}, \qquad (3.7)$$

where the dielectric function is given by

$$\epsilon = \epsilon_b + L_{LFE}\chi. \qquad (3.8)$$

where ϵ_b is the inert background dielectric constant which is taken in this work as $\epsilon_b = 16$ of Ge [8]. By L_{LFE}, we include the surface polarization effects, also called local field effects (LFEs) to our calculations using a simple semiclassical model [9]. The effect is a result of the dielectric mismatch between the constituent NC and host matrix which lead to remarkably different optical properties. The correction factor L_{LFE} for a linear response is given by,

$$L_{LFE} = \frac{3\epsilon_h}{\epsilon_{NC} + 2\epsilon_h} \qquad (3.9)$$

NCs Diameter (nm)	Radiative Recombination Lifetimes (ns)
1.11	7.76
1.47	10.48
2.02	16.72
2.55	72.06
3.03	117.3

Table 3.1: The radiative lifetimes for different NCs diameters.

where ϵ_h and ϵ_{NC} are the dielectric functions of the host matrix and the NC with the values $\epsilon_h = 4$ and $\epsilon_{NC} = 16$, respectively [8]. The implementation assumes a static local field correction, otherwise it brings negative absorption regions at high energies [8].

As an application of slow light in nanocrystals, one can consider the heavy-hole (HH) exciton or the valence and conduction ground states as a two-level system of our previous discussions. In principle, as long as the optical transitions between these two-levels is dipole-allowed, CPO based slow light can be implemented for this system. We consider the latter, the HOMO and LUMO levels make up our two level system. We applied the previous theoretical discussions for these levels of Ge nanocrystals.

3.4   Relaxation and Dephasing Times in Ge NCs

Relaxation and dephasing times are very crucial inputs for the OBEs. In Eq. (2.55), $(\rho_{22} - \rho_{11})^{(eq)}$ is the equilibrium population inversion of the material in the thermal equilibrium. Since this is an equilibrium value the slowest relaxation mechanism determines the lifetime of excited level. In semiconductors, this process is the radiative recombination which is in the time range of nanoseconds [58]. By our group's previous works [55], the radiative recombination lifetimes have been calculated. Some of these values are given in Table 3.1.

3.5 Results

We study the dynamic evolution of the system by solving Eqs. (2.54) and (2.55) numerically with the initial conditions $\sigma_{11} = 1$, $\sigma_{22} = 0$ and $\sigma_{21} = \sigma_{12} = 0$. The time evolution of the population inversion is shown in Fig. 3.6. The oscillations in th
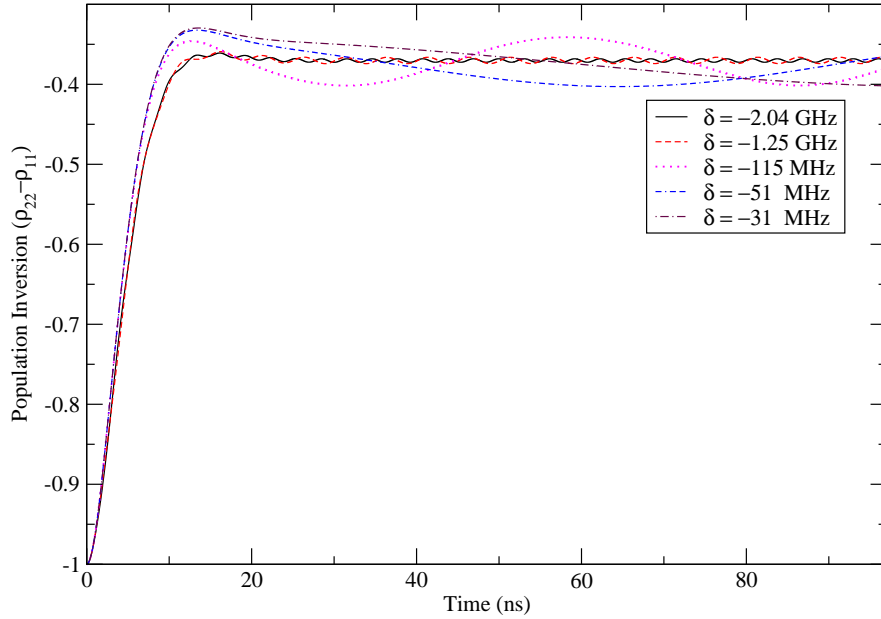
Figure 3.6: The coherent population oscillations for different detunings in the time domain for 1.47 nm diameter NCs with $\mathcal{E}_s = 200\ V/m$, $\mathcal{E}_p = 20\ V/m$, and $T_2/T_1 = 0.2$.

Initially for different parameter sets, we compared our numerical calculations with the analytical results. Figures 3.7 and 3.8 give examples of comparison for different arbitrary parameters for both imaginary and real parts of susceptibility, χ. There is a good agreement between the two solutions. Although, we always compared our numerical calculations with the analytical results, in the rest we are going to use our numerical method.

In Eq. (2.59), we derived the relation between T_1 and T_2. The dephasing process is very complicated due to intrinsic many-body effects. Hence, it is difficult

Figure 3.7: The comparison of numerical calculations with the analytical results
for arbitrary parameters. The absorption response with respect to detuning.

Figure 3.8: The comparison of numerical calculations with the analytical results
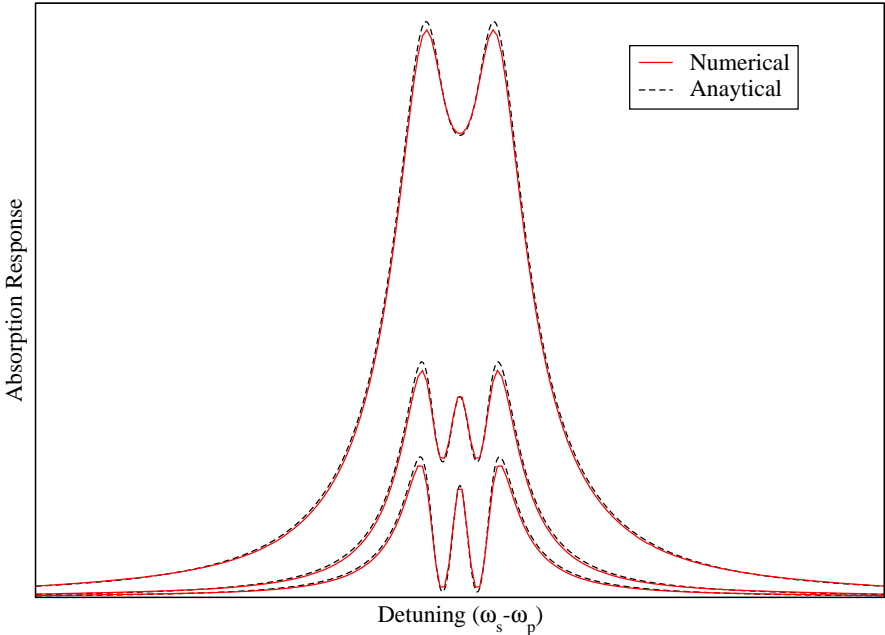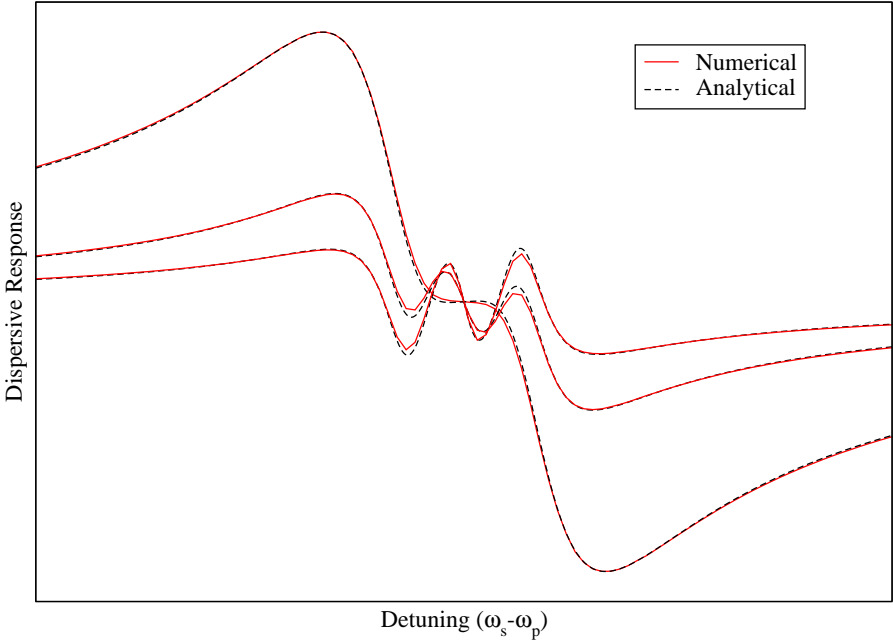for arbitrary parameters. The dispersive response with respect to detuning.
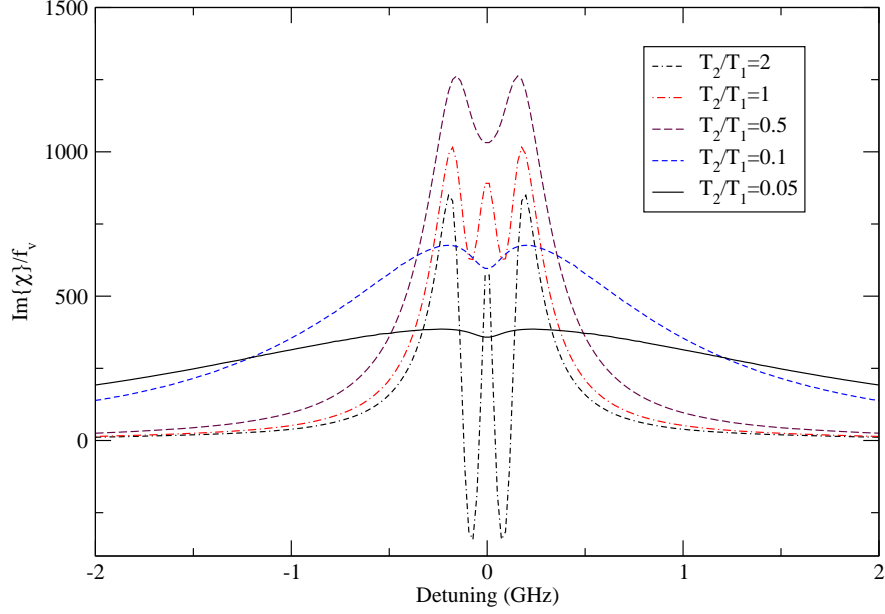
Figure 3.9: The absorptive response is given as a function of detuning and for different $\frac{T_2}{T_1}$. For 1.47 nm diameter NCs, $\mathcal{E}_s = 150 \ V/m$ and $\mathcal{E}_p = 15 \ V/m$.

to calculate dephasing times. In this manner, we prefer to give comparisons of different $\frac{T_2}{T_1}$ ratios by fixing T_1 at the radiative recombination time. Figure 3.9 gives the comparison for $\frac{T_2}{T_1}$ ratios. The main message of Fig. 3.9 is that the narrow dip that can produce slow-light is observed when $\frac{T_2}{T_1} < 0.5$.

Figure 3.10 illustrate the effect of the pump field, $\mathcal{E}_s$. We observe that by varying the power of pump field, we can alter the absorption curve. This is very important to produce controllable slow light. Figure 3.11 more explicitly illustrates that the slope of change of refractive index first increase with increasing pump field, then after some level again reduces.

After this first analysis, we can examine the slow light in Ge NCs via the slowdown factor. Hence, we follow the Eqs. (3.6-3.9) where the complex suscep-tibility, χ is defined in Eq. (3.10). In the definition of χ, we have N, the density of dipole moments. For the NCs, this value is the density of NCs. Since each computational supercell V_{SC} that we described in Part 3.1 contains just one NC,

Figure 3.10: The imaginary part of susceptibility, χ is given as a function of detuning and for different $\frac{\mathcal{E}_s}{\mathcal{E}_p}$. For 1.47 nm diameter NCs, fixing $\mathcal{E}_p = 15 \ V/m$.
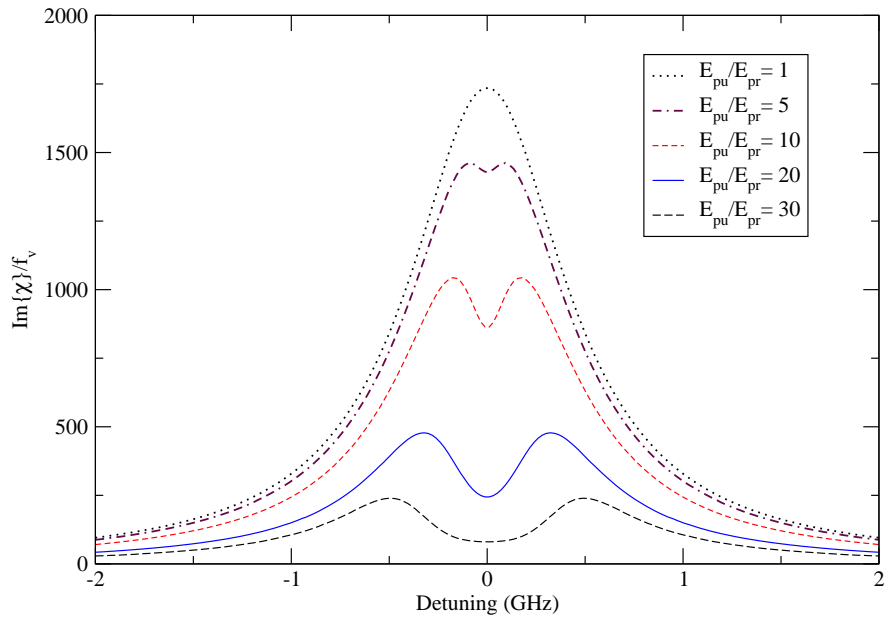

Figure 3.11: The real part of susceptibility is given as a function of detuning and for different $\frac{\mathcal{E}_s}{\mathcal{E}_p}$. For 1.47 nm diameter NCs, fixing $\mathcal{E}_p = 15 \ V/m$.
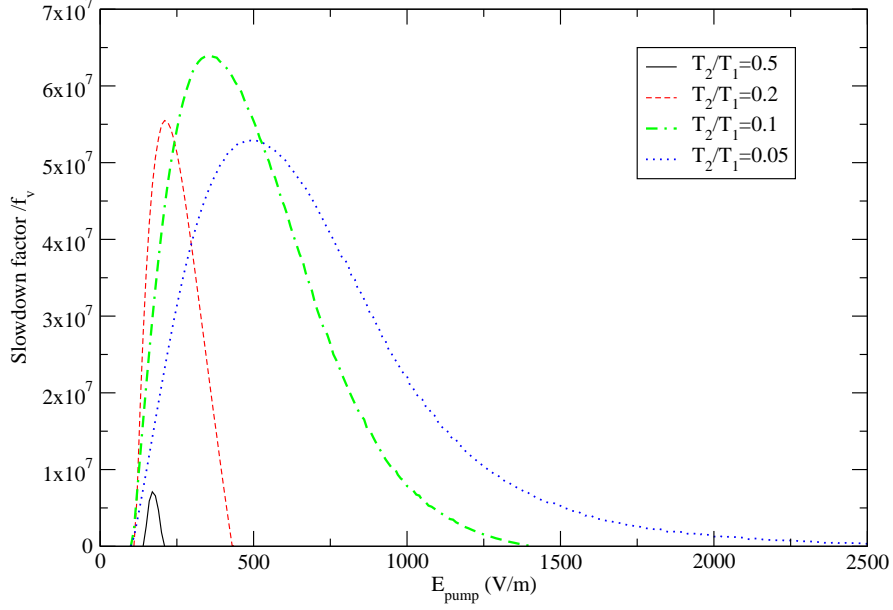
Figure 3.12: Slowdown factor versus the pump field intensity. For 1.47 nm diameter NCs, fixing $\mathcal{E}_p = 15 \ V/m$.

the value of N is equal to $1/V_{SC}$. Following Eq. (3.10), we write,

$$\tilde{\chi}(\omega) = \frac{[\rho_{12}(\omega)\vec{\mu}_{21} + \rho_{21}(\omega)\vec{\mu}_{12}]}{V_{SC}\epsilon_b \vec{\mathcal{E}}(\omega)} = \frac{V_{NC}}{V_{SC}} \frac{[\rho_{12}(\omega)\vec{\mu}_{21} + \rho_{21}(\omega)\vec{\mu}_{12}]}{V_{NC}\epsilon_b \vec{\mathcal{E}}(\omega)} \ . \tag{3.10}$$

where the filling factor, $f_v = \frac{V_{NC}}{V_{SC}}$ can be defined whih gives the volume filling ratio of the NC. This value can change between 0.05 to 0.1. For the sake of generality, this is the form we are presenting our results.

In Figure 3.12, for the 1.47 nm NCs, the slowdown factor, S is given with respect to the increasing pump field. For this NC, the bandgap is 2.54 nm and this gap requires the pump field with wavelength 488 nm. Comparison with respect to different dephasing times are also given in the same plot.

Next, in Fig. 3.13, we consider the nanocrystal with 2.01 nm diameter. The NC has 1.97 eV bandgap which corresponds to 630 nm wavelength for the coupled pump field. For this nanocrystal, the HOMO-LUMO transition electric dipole moments have very small values so that transition is very weak. Although, we pump the system with very large coupling fields, there is no significant slow

light effect for this nanocrystals if the pump and probe fields are just coupled to
HOMO-LUMO transition. For bigger NCs, for instance 2.55 nm, although we
tried different transitions beyond HOMO-LUMO, we have not manage to observe
effi
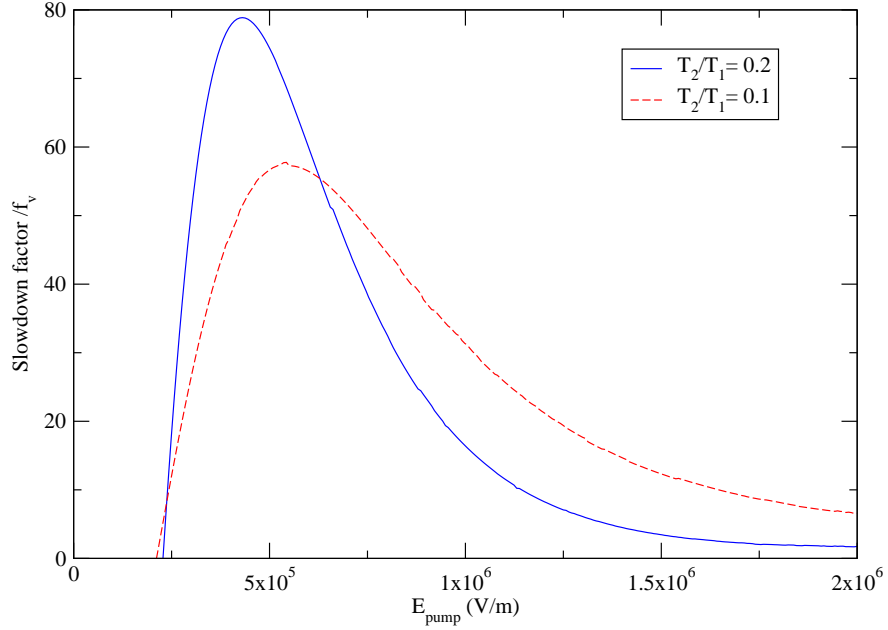
Figure 3.13: Slowdown factor versus the pump field intensity. For 2.01 nm diameter NCs, fixing $\mathcal{E}_s = 3000 \ V/m$.

The slowdown factor also sensitive to the phase difference bewteen the pump
and probe fields. Figure 3.14 illustrates this relation.

In CPO mechanism the absorption dip is determined by the inverse of the
population lifetime. In our calculations this value ranges in nanoseconds. Hence,
slow light produced in Ge NCs allow for operating bandwidths in the MHz-range.

CPO based slow light provides GHz bandwidths, if the lifetime is in the range
of picoseconds. Hence, if other faster recombination mechanisms rather than
radiative recombination are more effective in the population relaxation, then GHz
bandwidth can also be observed in Ge NCs. So actually our results here set a
lower limit to the bandwidth. A GHz value is much higher than those schemes
based on the other coherent control mechanisms in different material systems.
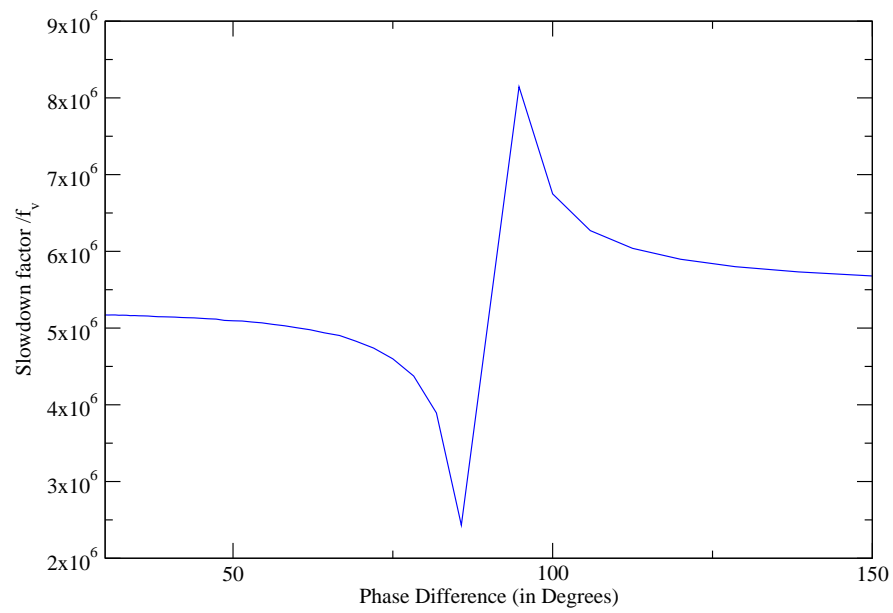
Figure 3.14: Slowdown factor versus the phase difference between the pump and probe fields.

Chapter 4

Semiconductor Bloch Equations

In the preceding chapter we analyzed the quantum-coherence effects via density matrix equations. That analysis is based on atomic quantum-coherence theory, where many-body effects are neglected. We just included phenomenological damping terms for dephasing and relaxation processes. A physically more realistic analysis should include the many-body Coulomb interactions since these strongly alter the optical properties of semiconductors. Some consequences of Coulomb interactions are renormalization of energies, i.e., reduction of band gap with increasing carrier density, redistribution of carriers, and enhancement of interband transitions by attractive electron-hole interactions. The Coulomb interactions are also responsible for the dephasing, which breaks the initially coherent excitations into incoherent superpositions. On the other hand, as a consequence of many-body effect, the plasma screening reduces the Coulomb interaction potential by the presence of background charge carriers. Thus, one can expect that the many-body effects will give rise to significant differences from the atomic theory [24, 25, 53].

In this chapter, we include many-body effects into our calculations to give a more realistic description. By this way, we also consider electron-hole plasma effects, band-filling dynamics and carrier-carrier collisions. All these phenomena can be described by the Semiconductor Bloch Equations (SBEs). There are two basic formulations to represent the SBEs. These are electron-hole formalism and

exciton-biexciton formalism. The latter formalism can be found in Ref. [24].
Here we apply the electron-hole formalism.

As we did in the preceding chapter, we start with the general formalism and
then discuss the coherent population oscillation mechanism but now for a multi-
level system. By comparing with the results of preceding chapter, one can illus-
trate the contributions of many-body effects.

4.1 General Formalism

The idea of SBEs is based on Bloch's work on the theory of nuclear spin reso-
nance [40] and Haken's laser theory [50]. For semiconductors, Haug et al. de-
rived the Bloch equations via nonequilibrium Green's function techniques [24],
whereas Koch and his colleagues derived these equations using quantum mechan-
ical projection-operator techniques [53]. During the last two decades SBEs have
became a key method in semiconductor optics [54].

In SBEs, it is convenient to exploit the electron-hole representation. By this
way, we avoid of discussing electrons in different states (bands). Instead we
introduce holes as missing electrons in the valence bands. Generally, for semi-
conductors in equilibrium the conduction bands are empty of electrons and the
valence band is totally full of electrons. Then an excited state is the promotion
of an electron from the valance band to conduction band, while leaving an hole
in the valence band.

We define operators for the quasi-particles conduction band electrons ($a^\dagger$, a)
and valence band holes ($b^\dagger$, b) via

$$
\begin{aligned}
a^\dagger_{\mathbf{k},s} &= a^\dagger_{c,\mathbf{k},s}, & a_{\mathbf{k},s} &= a_{c,\mathbf{k},s} \\
b_{-\mathbf{k},-s} &= a^\dagger_{v,\mathbf{k},s}, & b^\dagger_{-\mathbf{k},-s} &= a_{v,\mathbf{k},s}
\end{aligned}
$$

where, for instance, the last relation means that the annihilation of an electron
with momentum $\mathbf{k}$ and spin s in the valance band corresponds to the creation
of an hole with the opposite momentum and spin. Within this representation

we are going to obtain SBEs which are coupled differential equations coupling polarizations and electron, hole populations.

In order to discuss the optical properties of nanocrystals, we should solve the equation of motion for the polarization. The Hamiltonian of the problem should contain the kinetic energies of carriers, the interaction between the carriers and the external coherent field, and the many-body Coulomb interactions. To get rid of the complications of the complete theory, we introduce some approximations allowing us to begin with a tractable treatment which contains the most significant contributions, then we can gradually inject the missing parts.

The full formulation of many-body electron-hole plasma in the second quantization can be found in Haken's classical book Quantum Field Theory of Solids [49]. We just get here the required components.

The total Hamiltonian of an interacting electron-hole plasma in a nanocrystal structure coupled to external electromagnetic fields is given by

$$\mathcal{H} = \mathcal{H}_o + \mathcal{H}_{c-f} + \mathcal{H}_c, \tag{4.1}$$

where $\mathcal{H}_o$ and $\mathcal{H}_{c-f}$ are free-carrier contributions and $\mathcal{H}_c$ is the Coulomb interaction part. For free-carrier parts we assume that the carrier interactions are sufficiently rapid in comparison to the field transients, and the main effect of the Coulomb interactions on the carriers is to relax them within the bands to quasi-equilibrium Fermi-Dirac distributions; whence we treat the interactions as reservoir interactions establishing intraband quasi-equilibrium carrier distributions instead of dynamical interactions. This let us write the free-carrier kinetic energies

$$\mathcal{H}_o = \sum_n \varepsilon_n^e a_n^\dagger a_n + \sum_m \varepsilon_m^h b_m^\dagger b_m, \tag{4.2}$$

where εs are the free-carrier electron and hole energies. n and m indices denotes the corresponding energy levels.

The light-matter interaction can be again described by the dipole approximation, but now within the second quantized formalism,

$$\mathcal{H}_{c-f} = -\vec{\mathcal{E}}(t) \cdot \vec{\mathcal{P}} \tag{4.3}$$

where the interband polarization operator is given by

$$\vec{\mathcal{P}} = \sum_{n,m}(\vec{\mu}_{nm}a_n^\dagger b_m^\dagger + \vec{\mu}_{nm}^* b_m a_n) \tag{4.4}$$

here μ_{nm} is the dipole moment element between the corresponding energy levels $|n\rangle$ and $|m\rangle$. Then the interband dipole coupling to the light field is

$$\mathcal{H}_{c-f} = -\sum_{n,m}(\vec{\mu}_{nm}a_n^\dagger b_m^\dagger + \vec{\mu}_{nm}^* b_m a_n)\cdot\vec{\mathcal{E}}(t). \tag{4.5}$$

The last contribution to the total Hamiltonian is Coulomb interaction energy among the carriers,

$$\mathcal{H}_c = \frac{1}{2}\sum_{n,m,r,s}W_{nm}^{rs}a_r^\dagger a_s^\dagger a_m a_n + \frac{1}{2}\sum_{n,m,r,s}W_{nm}^{rs}b_r^\dagger b_s^\dagger b_m b_n - \sum_{n,m,r,s}W_{nm}^{rs}a_r^\dagger b_s^\dagger b_m a_n \tag{4.6}$$

which contains the Coulomb interactions among the electrons, among the holes and among the electrons and holes, respectively [49]. W_{nm}^{rs} is the Coulomb interaction energy matrix element

$$W_{nm}^{rs} = \int d^3r_1 d^3r_2 \phi_r^*(\mathbf{r}_1)\phi_n(\mathbf{r}_1)W(\mathbf{r}_1-\mathbf{r}_2)\phi_s^*(\mathbf{r}_2)\phi_m(\mathbf{r}_2) \tag{4.7}$$

where $\phi_n(\mathbf{r})$ is a wavefunction of the nanocrystal. The Coulomb potential is given by,

$$W(\mathbf{r}_1-\mathbf{r}_2) = \frac{e^2}{4\pi\epsilon_0\epsilon_b|\mathbf{r}_1-\mathbf{r}_2|} \tag{4.8}$$

The electric charge and vacuum dielectric constants are denoted by e and ϵ_0, respectively. For the background host material Ge NCs, the dielectric constant is $\epsilon_b = 16$ [9].

4.2 Multi-Level System

In our treatment of many-body effects, we apply semiclassical light-matter interaction theory. In semiclassical approach the carriers are treated quantum mechanically whereas the electromagnetic field is treated classically. As a generalization of Eq. (2.11), the microscopic optical properties are linked to the macroscopic optical properties via the optical polarization,

$$\vec{P}(t) = N_{nx}\sum_{i,j}p_{ij}(t)\vec{\mu}_{ij} \tag{4.9}$$

where $\vec{\mu}_{ij}$ are the electric dipole moments and p_{ij} are the corresponding density matrix elements [24].

The quantum mechanical operators corresponds to the observables of classical physics. Since the operators are time-dependent in the Heisenberg picture as the classical observables, the link between the quantum and classical theories can be most easily formed within this picture. If we are solving the Schrödinger equation,

$$i\hbar\frac{\partial}{\partial t}\Psi(t) = \mathcal{H}\Psi(t), \tag{4.10}$$

then in the Heisenberg picture for the time evolution of the system, we write

$$\Psi(t) = U_H\Psi_H(0) \quad with \quad U_H = e^{-\frac{i}{\hbar}\mathcal{H}t} \tag{4.11}$$

which manifests that in this picture the time dependence is completely transferred to the operators from the wave functions. The operators are transformed according to

$$\mathcal{A}_H = U_H^\dagger \mathcal{A} U_H = e^{\frac{i}{\hbar}\mathcal{H}t}\mathcal{A}e^{-\frac{i}{\hbar}\mathcal{H}t} \tag{4.12}$$

taking the derivatives of both sides with respect to time,

$$\frac{d}{dt}\mathcal{A}_H = -\frac{i}{\hbar}(\mathcal{A}_H\mathcal{H} - \mathcal{H}\mathcal{A}_H) + \frac{\partial}{\partial t}\mathcal{A}_H = -\frac{i}{\hbar}[\mathcal{A}, \mathcal{H}] + \frac{\partial}{\partial t}\mathcal{A}_H \tag{4.13}$$

This equation is called Heisenberg's equation of motion which describes the time evolution of operators in the Heisenberg picture. The term $\frac{\partial}{\partial t}\mathcal{A}_H$ refers to the explicit time dependence of operator $\mathcal{A}_H$.

Inserting the total Hamiltonian given by Eqs. (4.1) into Eq. (4.13) and by taking the expectations of both sides, we can derive the equations of motions for the polarizations and the electron and hole populations within the corresponding energy levels. For instance, for the interband polarization $p_{\beta\alpha} = \langle b_\beta a_\alpha\rangle$ we have the equation of motion

$$i\hbar\frac{d}{dt}b_\beta a_\alpha = [b_\beta, a_\alpha, \mathcal{H}_{tot}] \tag{4.14}$$

Initially we ignore the explicit time-dependence of operators which will be considered later.

In order to proceed the calculations, we should recall some useful identities. In the second quantization the wave function $\Psi(\mathbf{r})$ can be decomposed into a

complete othonormal set $|n\rangle$ as

$$\Psi(\mathbf{r}) = \sum_n a_n |n\rangle \tag{4.15}$$

and correspondingly

$$\Psi^\dagger(\mathbf{r}) = \sum_n a_n^\dagger \langle n| \tag{4.16}$$

The wave function describing the electrons and holes should obey the Pauli principle and so fermionic anti-commutation relations:

$$
\begin{aligned}
\Psi(\mathbf{r})\Psi^\dagger(\mathbf{r}') + \Psi^\dagger(\mathbf{r}')\Psi(\mathbf{r}) &= \delta(\mathbf{r} - \mathbf{r}') \\
\Psi(\mathbf{r})\Psi(\mathbf{r}') + \Psi(\mathbf{r}')\Psi(\mathbf{r}) &= 0 \\
\Psi^\dagger(\mathbf{r})\Psi^\dagger(\mathbf{r}') + \Psi^\dagger(\mathbf{r}')\Psi^\dagger(\mathbf{r}) &= 0
\end{aligned}
\tag{4.17}
$$

Inserting Eqs. (4.15) and (4.16) into these equations, we get the following anti-commutation relations for the electron operators a and $a^\dagger$:

$$
\begin{aligned}
a_n a_m^\dagger + a_m^\dagger a_n &= \{a_n, a_m^\dagger\} = \delta_{nm} \\
a_n a_m + a_m a_n &= \{a_n, a_m\} = 0 \\
a_n^\dagger a_m^\dagger + a_m^\dagger a_n^\dagger &= \{a_n^\dagger, a_m^\dagger\} = 0
\end{aligned}
\tag{4.18}
$$

and the same relations for the hole operators b and $b^\dagger$. We should also use the following commutation identities for the right hand sides of equation of motions,

$$
\begin{aligned}
[A, BC] &= [A, B]C + B[A, C] \\
[AB, C] &= A\{B, C\} - \{A, C\}B
\end{aligned}
$$

combining these two identity for two-by-two commutators we obtain:

$$
\begin{aligned}
[AB, CD] &= [AB, C]D + C[AB, D] \\
&= A\{B, C\}D - \{A, C\}BD + CA\{B, D\} - C\{A, D\}B \tag{4.19}
\end{aligned}
$$

and for two-by-four commutators we obtain:

$$[AB, CDEF] = [AB, CD]EF + CD[AB, EF]. \tag{4.20}$$

We can use these identities with the anti-commutation relations Eq. (4.18) to derive the equations of motions.

As one should notice or explicitly see in the Appendix part when we insert Eq. (4.19) in the right hand side of Eq. (4.20), the product of two particle operators are coupling to the products of four particle operators. Similarly, four operator is in turn coupled to six operator, and so on. This will cause an infinite hierarchy of coupled differential equations. In order to truncate this hierarchy, we factorize the higher-order expectation values into products of second-order averages, $p_{\alpha\beta} = \langle b_\beta a_\alpha \rangle$, $n_\alpha^e = \langle a_\alpha^\dagger a_\alpha \rangle$ and $n_\beta^h = \langle b_\beta^\dagger b_\beta \rangle$. This is done by factorizing the four-operator expectation values into all possible operator combinations leading to products of polarizations and/or populations. There are several examples of factorization in the Appendix. This approach is called the Hatree-Fock factorization since Hartree and Fock made a similar approximation while studying the many-electron atom. Hartree-Fock approximation contains some Coulomb effects such as bandgap renormalization and interband Coulomb enhancement; nevertheless, omits some further renormalization and collision terms. The most important of them are the screening and connected renormalizations, as well as electron-electron, electron-hole and hole-hole scattering, and polarization dephasing. We also know that, in addition to the Coulombic interactions included to the total Hamiltonian, there are other scattering and dephasing mechanisms, such as carrier-phonon interactions and scattering by impurities and imperfections of the material [25]. For a more accurate discussion, we should add all these missing parts while considering the explicit time-dependence of operators.

For the interband electron-hole transitions connecting states $|e1\rangle$ and $|h1\rangle$, Eq. (A.3) in the Appendix gives,

$$
\begin{aligned}
\frac{\partial}{\partial t} p_{e1h1} &= -i\omega_{e1h1}^{(0)} p_{e1h1} + i\Omega_{e1h1} - i\sum_\beta \Omega_{e1\beta} p_{\beta h1} - i\sum_\alpha \Omega_{\alpha h1} p_{\alpha e1} \\
&+ i\sum_\alpha \Delta_{\alpha e1}^e p_{\alpha h1} + i\sum_\beta \Delta_{\beta h1}^h p_{e1\beta} + \frac{\partial p_{e1h1}}{\partial t}\bigg|_{col}.
\end{aligned} \tag{4.21}
$$

where $\hbar\omega_{\alpha\beta}^{(0)} = \varepsilon_\alpha^e + \varepsilon_\beta^h$ and ε_α^e and ε_β^h are single particle electron and hole energy levels. Similarly, Eqs. (A.6) and (A.9) of Appendix become,

$$
\begin{aligned}
\frac{\partial}{\partial t} p_{e1e2} &= -i\omega_{e1e2}^{(0)} p_{e1e2} + i\sum_\beta \Omega_{e2\beta} p_{e1\beta}^* - i\sum_\beta \Omega_{e1\beta}^* p_{e2\beta} \\
&+ i\sum_\alpha \Delta_{\alpha e2}^e p_{e1\alpha} - i\sum_\alpha \Delta_{\alpha e1}^{e*} p_{\alpha e2} + \frac{\partial p_{e1e2}}{\partial t}\bigg|_{col}.
\end{aligned} \tag{4.22}
$$

and

$$\frac{\partial}{\partial t}p_{h1h2} = -i\omega_{h1h2}^{(0)}p_{h1h2} + i\sum_{\alpha}\Omega_{\alpha h2}p_{\alpha h1}^* - i\sum_{\alpha}\Omega_{\alpha h1}^*p_{\alpha h2}$$

$$+ i\sum_{\beta}\Delta_{\beta h2}^h p_{h1\beta} - i\sum_{\beta}\Delta_{\beta h1}^{h*}p_{\beta h2} + \frac{\partial p_{h1h2}}{\partial t}\bigg|_{col}. \qquad (4.23)$$

where $\hbar\omega_{\alpha\alpha'}^{(0)} = \varepsilon_{\alpha'}^e - \varepsilon_\alpha^e$, $\hbar\omega_{\beta\beta'}^{(0)} = \varepsilon_{\beta'}^h - \varepsilon_\beta^h$. These equations are written in a general form such that, for instance, p_{e1e2} gives the intraband polarization if $e1 \neq e2$ and otherwise gives the population distribution $p_{e1e2} = n_{e1} = \langle a_{e1}^\dagger a_{e1}\rangle$ for the level $|e1\rangle$ if $e1 = e2$.

In order to write these equations compactly, we defined the generalized Rabi frequency,

$$\hbar\Omega_{\alpha\beta} = \vec{\mu}_{\alpha\beta} \cdot \vec{\mathcal{E}}(t) + \sum_{\alpha',\beta'} W_{\alpha'\beta'}^{\alpha\beta} p_{\alpha'\beta'}, \qquad (4.24)$$

and the many-body Coulomb interactions are grouped in the electron and hole terms $\Delta_{\alpha e1}^e$ and $\Delta_{\beta h1}^h$, respectively:

$$\hbar\Delta_{\alpha e1}^e = \sum_{\alpha',\alpha''}\left(W_{\alpha\alpha''}^{\alpha'e1} - W_{\alpha''\alpha}^{\alpha'e1}\right)p_{\alpha'\alpha''} + \sum_{\beta,\beta'}W_{\alpha\beta'}^{e1\beta}p_{\beta\beta'} \qquad (4.25)$$

$$\hbar\Delta_{\beta h1}^h = \sum_{\beta',\beta''}\left(W_{\beta\beta''}^{\beta'h1} - W_{\beta''\beta}^{\beta'h1}\right)p_{\beta'\beta''} + \sum_{\alpha,\alpha'}W_{\alpha'\beta}^{\alpha h1}p_{\alpha\alpha'} \qquad (4.26)$$

The Coulomb interactions between valence holes and conduction electrons reduce the optical transition energy with increasing carrier density. This effect is called *bandgap renormalization*. To observe the bandgap renormalization we separate the $e1$ and $h1$ terms from the sums. Thus the bandgap renormalization is,

$$\omega_{e1h1} = \omega_{e1h1}^{(0)} + \Delta_{e1e1}^e + \Delta_{h1h1}^h \qquad (4.27)$$

since Eq. (4.21) is now in the form of,

$$\frac{\partial}{\partial t}p_{e1h1} = -i\omega_{e1h1}p_{e1h1} + i\Omega_{e1h1} - i\sum_{\beta}\Omega_{e1\beta}p_{\beta h1} - i\sum_{\alpha}\Omega_{\alpha h1}p_{\alpha e1}$$

$$+ i\sum_{\alpha\neq e1}\Delta_{\alpha e1}^e p_{\alpha h1} + i\sum_{\beta\neq h1}\Delta_{\beta h1}^h p_{e1\beta} + \frac{\partial p_{e1h1}}{\partial t}\bigg|_{col}. \qquad (4.28)$$

These equations explicitly contains the Hartree-Fock contribution terms whereas all correlations beyond Hartree-Fock are grouped in the collision contributions and denoted as $\frac{\partial}{\partial t}|_{col}$. As an improvement to the Hartree-Fock approximation, we may utilize the next level Coulombic contributions to the carrier scattering and dephasing which yields the collision terms. We can write this approximation, for instance, for a two-operator combination ab,

$$
\begin{aligned}
\frac{d}{dt}\langle ab\rangle &= \frac{d}{dt}\langle ab\rangle_{HF} + \left(\frac{d}{dt}\langle ab\rangle - \frac{d}{dt}\langle ab\rangle_{HF}\right) \\
&\equiv \frac{d}{dt}\langle ab\rangle_{HF} + \frac{d}{dt}\langle ab\rangle_{col}
\end{aligned}
$$

where HF denotes the Hartree-Fock contribution [25]. In order to get a better approximation we should have a satisfactory estimation about the collision contributions and we should add up that into our calculations.

In semiconductors actual dephasing mechanisms should be considered in the context of quantum kinetic theory [25]. However, such treatment will be very complicated and more significantly very expensive in terms of computation time. In such a treatment, it is very difficult to give comparisons for different system configurations as we do in Chapter 3. So we prefer an effective rate approximation.

For the nondiagonal density matrix elements, i.e., the polarizations, the collision effects are approximated by an effective dephasing rate [23],

$$
\left.\frac{\partial p_{ij}}{\partial t}\right|_{col} = -\gamma_p p_{ij}
$$

As we mentioned in the introduction part, the main result of carrier-carrier scattering is to drive the electron and hole distributions within their bands to Fermi-Dirac distributions. These distributions are called quasi-equilibrium distributions. Quasi-equilibrium distributions occurs on a time scale longer than the carrier-carrier scattering time of tens of femtoseconds and shorter with respect to interband relaxation time of nanoseconds [25].

This rapid carrier equilibration gives rise to Fermi-Dirac distributions for the

energy level i,

$$f_i = \frac{1}{\exp\left(\dfrac{\varepsilon_i - \mu_j^p}{k_B T_p}\right) + 1} = f_i(\mu_j^p, T_p),$$

where j is $e(h)$ for electrons (holes). μ_j^p is called the plasma quasi-chemical potential and T_p is the plasma temperature [23].

To follow the convention let us write for the electron states, $p_{\alpha\alpha} = n_\alpha$. Then the relaxation process for the diagonal density matrix elements, i.e., the population distributions are given by,

$$\left.\frac{\partial n_\alpha}{\partial t}\right|_{col} = -\gamma_r n_\alpha - \gamma_{c-c}[n_\alpha - f_\alpha(\mu_e^p, T_p)] - \gamma_{c-p}[n_\alpha - f_\alpha(\mu_e^l, T_l)]$$

where the carrier-phonon scatterings are also treated by the quasi-equilibrium Fermi-Dirac distributions. The μ_i^l is the lattice quasi-chemical potential and T_l is the lattice temperature. γ_r, γ_{c-c} and γ_{c-p} are the effective recombination, carrier-carrier and carrier-phonon collision rates, respectively. The same relations hold for the hole states; just the character e changes with h [23, 25].

γ_r corresponds to the usual recombination rate which can be taken from Table 3.1. γ_{c-c} and γ_{c-p} terms give in which rate the populations converge to quasi-equilibrium Fermi-Dirac distributions. For the carrier-carrier dynamics the dephasing rate $\gamma_{c-c} = 8 \times 10^{12}\ s^{-1}$ is reported in the literature for Ge NCs [51]. γ_{c-p} can roughly be taken in the same order.

While solving the system, at each time step the values of the chemical potentials and temperatures can be calculated from the following relations:

Total electron and hole populations are conserved in carrier-carrier collisions. Thus,

$$\sum_\alpha n_\alpha = \sum_\alpha f_\alpha(\mu_e^p, T_p)$$
$$\sum_\beta n_\beta = \sum_\beta f_\beta(\mu_h^p, T_p),$$

where the summations α and β are over all electron and hole states, respectively.

The third relation is the conservation of total electron and hole energies in carrier-carrier collisions,

$$\sum_\alpha \varepsilon_\alpha n_\alpha + \sum_\beta \varepsilon_\beta n_\beta = \sum_\alpha \varepsilon_\alpha f_\alpha(\mu_e^p, T_p) + \sum_\beta f_\beta(\mu_h^p, T_p)$$

where ε_α and ε_β are the energy levels for the electron and hole states, respectively.

For the carrier-phonon collisions, the total electron and hole populations are again conserved. Hence,

$$\begin{aligned}
\sum_\alpha n_\alpha &= \sum_\alpha f_\alpha(\mu_e^l, T_l) \\
\sum_\beta n_\beta &= \sum_\beta f_\beta(\mu_h^l, T_l),
\end{aligned}$$

and T_l is taken as the medium temperature [23, 25].

Hence, we finished to construct the SBEs. Although, SBEs derived so far can be solved in those forms, it is convenient to introduce new slowly varying variables as we described in the Chapter 2. With newly defined variables, we can see how we should apply the rotating wave approximation (RWA) and whence we significantly reduce the computation time. Since now the solver does not need to follow very rapidly oscillating terms with very short time step increments.

We see from Eqs. (4.21 - 4.23) that the nondriven [i.e., $\mathcal{E}(t) = 0$] and non-Columbic [i.e., $W_{ij}^{kl} = 0$] behavior of operators are,

$$\begin{aligned}
\rho_{\alpha\beta}(t) &= \rho_{\alpha\beta}(0)e^{-i\omega_{\alpha\beta}t} \\
\rho_{\beta\beta'}(t) &= \rho_{\beta\beta'}(0)e^{-i\omega_{\beta'\beta}t} \\
\rho_{\alpha\alpha'}(t) &= \rho_{\alpha\alpha'}(0)e^{-i\omega_{\alpha'\alpha}t},
\end{aligned} \tag{4.29}$$

observing these equations, let us define new slowly varying variables $\sigma_{\alpha\beta}$, $\sigma_{\beta\beta'}$ and $\sigma_{\alpha\alpha'}$ such that

$$\begin{aligned}
\rho_{\alpha\beta}(t) &= \sigma_{\alpha\beta}(t)e^{-i\omega_{\alpha\beta}t} \\
\rho_{\beta\beta'}(t) &= \sigma_{\beta\beta'}(t)e^{-i\omega_{\beta'\beta}t} \\
\rho_{\alpha\alpha'}(t) &= \sigma_{\alpha\alpha'}(t)e^{-i\omega_{\alpha'\alpha}t},
\end{aligned} \tag{4.30}$$
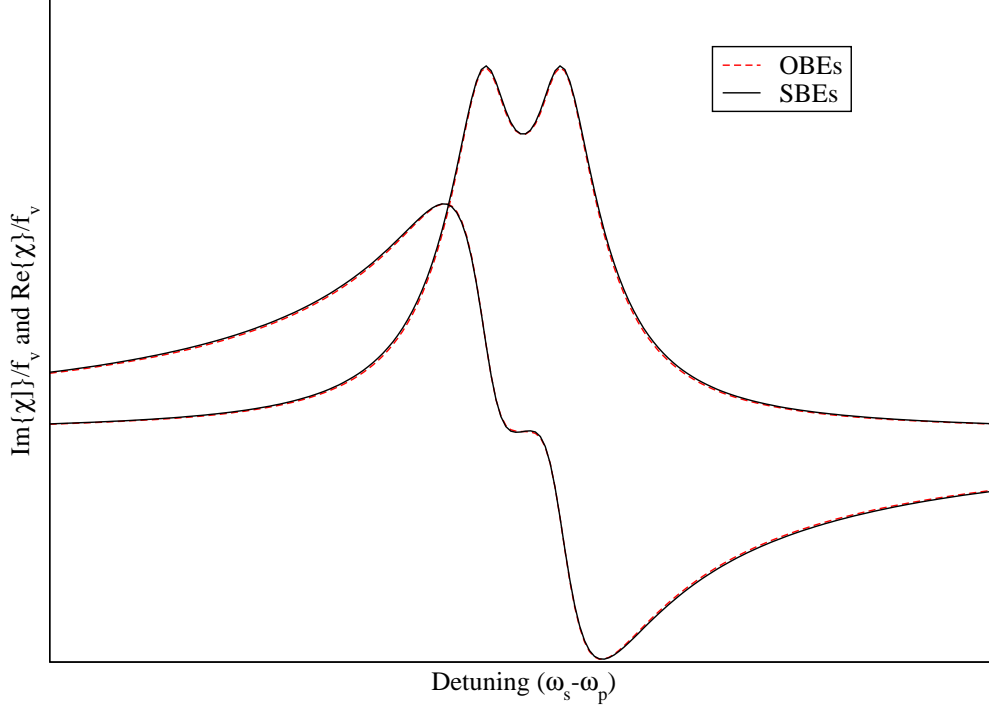
Figure 4.1: Comparison of OBEs and SBEs when there is no Coulomb interaction to check the code implementation.

By inserting these definitions into SBEs, we can again apply the RWA and ignore the rapidly oscillating exponential terms $e^{\pm i\omega t}$ with the frequency $\omega \approx 2\omega_{gap}$.

Now we are ready to solve SBEs. In our calculations we applied the pump field resonant with HOMO-LUMO transition and the probe field scanned around the pump field.

While starting many-body calculations, we initially checked our code by comparing with the results of OBEs. For a two-level system of HOMO-LUMO levels, we set the Coulomb interactions equal to zero. Since there are no many-body effects, we also took the γ_{c-c} and γ_{c-p} rates equal to zero. Further, we assumed that the population of excited level relaxes with radiative recombination process and the polarization dephases with time $T_2 = T_1/2$. This means we took same relaxation and dephasing times for both OBEs and SBEs. Fig. 4.1 illustrates that under these assumptions with any arbitrary parameters both solutions exactly coincide.

Solving SBEs is not a simple task. Since the carrier-carrier interactions are very rapid the quantum coherence effects also vanishes very rapidly. Although, in the atomic treatment the coherence effects observed in microsecond time ranges, now the effects maintains from tens of femtoseconds to picoseconds. To obtain stable results and give satisfactory comparisons further work is required.

Chapter 5

Conclusions and Future Work

In this thesis, we studied the coherent population oscillation based slow light in Ge NCs. Optical Bloch equations are derived and solved numerically considering a two-level scheme. The key point in our solution was that we have not used the fundamental approximation of analytical solution and obtained our results numerically. The numerical results are compared with the available analytical approach. A good agreement between them is observed. An analysis of outputs is given briefly and the slow light in Ge NCs is discussed.

Later, the carrier-carrier Coulomb interactions are included to the discussion. Semiconductor Bloch equations are derived where the carrier-carrier interactions are included at the level of Hartree-Fock approximation. Further interaction effects are included in the context of effective rate approximations. Further studies should be done to explore the many-body effects in the NCs systems.

Bibliography

[1] T. Tagahara (Ed.), *Quantum Coherence, Correlation and Decoherence in Semiconductor Nanostructures*, Academic Press, 2003.

[2] U. Woggon, *Optical Properties of Semiconductor Quantum Dots*, Springer-Verlag, Berlin, 1997.

[3] D. Bimberg, M. Grundmann, and N.N. Ledentsov, *Quantum Dot Heterostructures*, Wiley, West Sussex, 1999.

[4] H.F. Hess, E. Betzig, T.D. Harris, L.N. Pfeiffer, and K.W. West, Science **264**, 1740 (1994).

[5] D. Gammon, E.S. Snow, B.V. Shanabrook, D.S. Katzer, and D. Park, Science **273**, 87 (1996).

[6] K. Brunner, G. Abstreiter, G. Böhm, G. Trankle, and G. Weimann, Phys. Rev. Lett. **73**, 1138 (1994).

[7] P.W. Milonni, *Fast Light, Slow Light and Left-Handed Light*, IOP Publishing, Cornwall, 2005.

[8] H. Yıldırım and C. Bulutay, Phys. Rev. B **78**, 115307 (2008).

[9] C. Bulutay, Phys. Rev. B **76**, 205321 (2007).

[10] C. J. Chang-Hasnain, P. C. Ku, J. Kim, and S. L. Chuang, Proc. IEEE **91**, 1884 (2003).

[11] R.W. Boyd, *Nonlinear Optics*, Academic Press, Burlington, 2008.

[12] G.S. Agarwal and T.N. Dey, Laser & Photon. Rev. **3**, 287 (2009).

[13] S.E. Harris, J.E. Field, and A. Kasapi, Phys. Rev. A **46**, R29 (1992).

[14] L.V. Hau, S.E. Harris, Z. Dutton, and C.H. Behroozi, Nature **397**, 594 (1999).

[15] M.M. Kash, V.A. Sautenkov, A.S. Zibrov, L. Hollberg, G.R. Welch, M.D. Lukin, Y. Rostovtsev, E.S. Fry, and M.O. Scully, Phys. Rev. Lett. **82**, 5229 (1999)

[16] A. Kasapi, M. Jain, G. Y. Yin, and S. E. Harris, Phys. Rev. Lett. **74**, 2447 (1995)

[17] D. Budker, D. F. Kimball, S. M. Rochester, and V. V. Yashchuk, Phys. Rev. Lett. **83**, 1767 (1999)

[18] M.S. Bigelow, N.N. Lepeshkin, and R.W. Boyd, Phys. Rev. Lett. **90**, 113903 (2003).

[19] P-C. Ku, F. Sedgwick, C.J. Chang-Hasnain, P. Palinginis, T. Li, H. Wang, S-W. Chang, and S-L. Chuang, Opt. Lett. **29**, 2291 (2004).

[20] H. Su and S-L. Chuang, Opt. Lett. **31**, 271 (2006).

[21] S-W. Chang, P.K. Kondratko, H. Su, and S.L. Chuang, Quantum Electronics, IEEE Journal of , **43**, 196-205 (2007).

[22] M.S. Bigelow, N.N. Lepeshkin, and R.W. Boyd, Science **301**, 200 (2003).

[23] W.W. Chow, H.C. Schneider, and M.C. Phillips, Phys. Rev. A **68** 053802 (2003).

[24] H. Haug and S.W. Koch, *Quantum Theory of the Optical and Electronic Properties of Semiconductors* , World Scientific Publishing, Singapore, 2004.

[25] W.W. Chow and S.W. Koch, *Semiconductor-Laser Fundamentals*, Springer-Verlag, Berlin, 1999.

[26] S. E. Schwarz and T. Y. Tan, Appl. Phys. Lett. **10**, 4 (1967).

[27] R. W. Boyd, M. G. Raymer, P. Narum, and D. J. Harter, Phys. Rev. A **24**, 411 (1981).

[28] R.L. Burden and J.D. Faires, *Numerical Analysis*, Brooks Cole, California, 2001.

[29] A. Yariv, *Quantum Electronics*, Wiley, New York, 1989.

[30] A.E. Siegman, *Lasers*, University Science Books, California, 1986.

[31] W. Demtröder, *Laser Spectroscopy*, Springer-Verlag, Heidelberg, 2003.

[32] W.S.C. Chang, *Principles of Laser and Optics*, Cambridge Uni. Press, Cambridge, 2005.

[33] B.H. Soffer and B.B. McFarland, Appl. Phys. Lett. **8**, 166 (1966).

[34] R.W. Boyd and S. Mukamel, Phys. Rev. A **29**, 1973 (1984).

[35] L. W. Hillman, R.W. Boyd, J. Krasinski, and C.R. Stroud, Opt. Commun. **45**, 416 (1983).

[36] M.G. Payne, L. Deng, and K.J. Jiang , Phys. Rev. A **74**, 043810 (2006).

[37] S. Mukamel, *Principles of Nonlinear Optical Spectroscopy*, Oxford University Press, Oxford, 1995.

[38] P. Meystre and M. Sargent III, *Elements of Quantum Optics*, Springer-Verlag, Heidelberg, 2007.

[39] M. Dressel and G. Grüner, *Electrodynamics of Solids*, Cambridge University Press, Cambridge, 2003.

[40] C. Kittel, *Introduction to Solid State Physics*, Wiley, New York, 2005.

[41] V. Vedral, *Modern Foundations of Quantum Optics*, Imperial College Press, London, 2005.

[42] T. Meier, P. Thomas, and S.W.Koch, *Coherent Semiconductor Optics*, Springer-Verlag, Heidelberg, 2007.

[43] M.O. Scully and M.S. Zubairy, *Quantum Optics*, Cambridge University Press, Cambridge, 1997.

[44] L.-W. Wang and A. Zunger, Phys. Rev. B **59** 15806 (1999).

[45] J.R. Chelikowsky and M.L. Cohen, Phys. Rev. B **14**, 556 (1976).

[46] M.L. Cohen and J.R. Chelikowsky, *Electronic Structure and Optical Properties of Semiconductors*, Springer-Verlag, Berlin, 1988.

[47] C. Bulutay, Phys. Rev. B **76** 205321 (2007).

[48] R.Y. Chiao and A.M. Steinberg, Progress in Optics XXXVII, edited by E. Wolf, Elsever, Amsterdam, 1997.

[49] H. Haken, *Quantum Field Theory of Solids*, North-Holland Publishing Company, Amsterdam, 1976.

[50] H. Haken, *Laser Theory*, Springer-Verlag, Berlin, 1984.

[51] S. Huang, H. Zhou, Z. Jiang, and F. Lu, Nanotechnology **16**, 53 (2005)

[52] F. Wooten, *Optical Properties of Solids* , Academic Press, New York City, 1972.

[53] T. Meier, P. Thomas, S.W. Koch, *Coherent Semiconductor Optics*, Springer-Verlag, Berlin, 2006.

[54] Kong-Thon Tsen (Ed.), *Ultrafast Dynamical Processes in Semiconductors*, Springer-Verlag, Berlin, 2004.

[55] C. Sevik, unpublished Ph.D. Thesis, Bilkent University, Ankara, 2008.

[56] T.R. Nielsen, Ph.D. Thesis, Institute for Theoretical Physics, University of Bremen, Germany, 2005; URL: http://elib.suub.uni-bremen.de/diss/docs/0010001.pdf.

[57] N. Baer, C. Gies, J. Wiersig, and F. Jahnke, Eur. Phys. J. B **50**, 411 (2006).

[58] P. Borri and W. Langbein in *Single Quantum Dots*, P. Michler (Ed.), p. 237-270, Springer-Verlag, Berlin, 2003.

Appendix A

Derivations of the Semiconductor Bloch Equations

The Hamiltonian of an interacting electron-hole plasma in a nanocrystal structure coupled to a coherent light field is given in the main text by Eq. (4.1). Inserting that Hamiltonian into the Heisenberg equation Eq. (4.13), we get the equation of motion for the polarization, $p_{e1h1} = \langle b_{h1}a_{e1}\rangle$ connecting the states $|e1\rangle$ and $|h1\rangle$,

$$i\hbar\frac{\partial}{\partial t}b_{h1}a_{e1} = [b_{h1}a_{e1}, \mathcal{H}]\,. \tag{A.1}$$

The commutation in the right hand side can be calculated explicitly using the commutation relations given in Eqs. (4.18-4.20),

$$
\begin{aligned}
[b_{h1}a_{e1}, a_n^\dagger a_n] &= [b_{h1}a_{e1}, a_n^\dagger]a_n + a_n^\dagger[b_{h1}a_{e1}, a_n]\\
&= b_{h1}\{a_{e1}, a_n^\dagger\}a_n - \{b_{h1}, a_n^\dagger\}a_{e1}a_n + a_n^\dagger b_{h1}\{a_{e1}, a_n\} - a_n^\dagger\{b_{h1}, a_n\}a_{e1}\\
&= \delta_{e1n}b_{h1}a_n\,,
\end{aligned}
$$

$$[b_{h1}a_{e1}, b_m^\dagger b_m] = -\{b_{h1}, b_m^\dagger\}a_{e1}b_m = -\delta_{h1m}a_{e1}b_m\,,$$

$$
\begin{aligned}
[b_{h1}a_{e1}, a_n^\dagger b_m^\dagger] &= b_{h1}\{a_{e1}, a_n^\dagger\}b_m^\dagger - a_n^\dagger\{b_{h1}, b_m^\dagger\}a_{e1}\\
&= \delta_{e1n}b_{h1}b_m^\dagger - \delta_{h1m}a_n^\dagger a_{e1}\,,
\end{aligned}
$$

$$[b_{h1}a_{e1}, b_m a_n] = 0\,,$$

$$[b_{h1}a_{e1}, a_r^\dagger a_s^\dagger \, a_m a_n] \; = \; [b_{h1}a_{e1}, a_r^\dagger a_s^\dagger] a_m a_n + a_r^\dagger a_s^\dagger [b_{h1}a_{e1}, a_m a_n]$$

$$= \; b_{h1}\{a_{e1}, a_r^\dagger\} a_s^\dagger a_m a_n + a_r^\dagger b_{h1}\{a_{e1}, a_s^\dagger\} a_m a_n$$

$$= \; \delta_{e1r} b_{h1} a_s^\dagger a_m a_n + \delta_{e1s} a_r^\dagger b_{h1} a_m a_n \,,$$

$$[b_{h1}a_{e1}, b_r^\dagger b_s^\dagger b_m b_n] \; = \; [b_{h1}a_{e1}, b_r^\dagger b_s^\dagger] b_m b_n + b_r^\dagger b_s^\dagger [b_{h1}a_{e1}, b_m b_n]$$

$$= \; -\{b_{h1}, b_r^\dagger\} a_{e1} b_s^\dagger b_m b_n - b_r^\dagger \{b_{h1}, b_s^\dagger\} a_{e1} b_m b_n$$

$$= \; -\delta_{h1r} a_{e1} b_s^\dagger b_m b_n - \delta_{h1s} b_r^\dagger a_{e1} b_m \,, b_n$$

$$[b_{h1}a_{e1}, a_r^\dagger b_s^\dagger b_m a_n] \; = \; [b_{h1}a_{e1}, a_r^\dagger b_s^\dagger] b_m a_n + a_r^\dagger b_s^\dagger [b_{h1}a_{e1}, b_m a_n]$$

$$= \; b_{h1}\{a_{e1}, a_r^\dagger\} b_s^\dagger b_m a_n - a_r^\dagger \{b_{h1}, b_s^\dagger\} a_{e1} b_m a_n$$

$$= \; \delta_{e1r} b_{h1} b_s^\dagger b_m a_n - \delta_{h1s} a_r^\dagger a_{e1} b_m a_n \,,$$

We insert all these commutation terms back into Eq. (A.1) and sum over corresponding indices in order to get rid of Kronecker δ-functions,

$$i\hbar \frac{\partial}{\partial t} b_{h1} a_{e1} \; = \; \varepsilon_{e1}^e b_{h1} a_{e1} - \varepsilon_{h1}^h a_{e1} b_{h1}$$

$$- \; \sum_m \vec{\mu}_{e1m} \cdot \vec{\mathcal{E}}(t)(\delta_{mh1} - b_{m}^\dagger b_{h1}) + \sum_n \vec{\mu}_{nh1} \cdot \vec{\mathcal{E}}(t) a_n^\dagger a_{e1}$$

$$+ \; \frac{1}{2} \sum_{n,m,s} W_{nm}^{e1s} b_{h1} a_s^\dagger a_m a_n + \frac{1}{2} \sum_{n,m,r} W_{nm}^{re1} a_r^\dagger b_{h1} a_m a_n$$

$$- \; \frac{1}{2} \sum_{n,m,s} W_{nm}^{h1s} a_{e1} b_s^\dagger b_m b_n - \frac{1}{2} \sum_{n,m,r} W_{nm}^{rh1} b_r^\dagger a_{e1} b_m b_n$$

$$- \; \sum_{n,m,s} W_{nm}^{e1s} b_{h1} b_s^\dagger b_m a_n + \sum_{n,m,r,s} W_{nm}^{rh1} a_r^\dagger a_{e1} b_m a_n \,.$$

If we concentrate on the first Coulomb interaction term, we notice that

$$\sum_{n,m,s} W_{nm}^{e1s} b_{h1} a_s^\dagger a_m a_n \; = \; \sum_{n,m,s} W_{mn}^{se1} b_{h1} a_s^\dagger a_m a_n = \sum_{n,m,r} W_{nm}^{re1} b_{h1} a_r^\dagger a_n a_m$$

$$= \; \sum_{n,m,r} W_{nm}^{re1} a_r^\dagger b_{h1} a_m a_n \,,$$

so its identical to the second term when we arranged dummy indices. In the first step we used $W_{nm}^{rs} = W_{mn}^{sr}$ property of the matrix element whereas in the last step we used the anti-commutation property in Eq. (4.18). Similarly, the third and fourth terms are same,

$$\sum_{n,m,s} W_{nm}^{h1s} a_{e1} b_s^\dagger b_m b_n \; = \; \sum_{n,m,s} W_{mn}^{sh1} a_{e1} b_s^\dagger b_m b_n = \sum_{n,m,r} W_{nm}^{rh1} a_{e1} b_s^\dagger b_n b_m$$

$$= \; \sum_{n,m,r} W_{nm}^{rh1} b_r^\dagger a_{e1} b_m b_n \,,$$

In the second quantization the multi-operator product expressions are written normal ordered, i.e., the creation operators are on the left of the annihilation operators. Such an ordering mechanism is crucial since by this way the unphysical interaction of a carrier by itself is excluded. For the fifth Coulomb interaction term, we apply the anti-commutation relation in order to obtain the normal ordering

$$b_{h1}b_s^\dagger b_m a_n = (\delta_{sh1} - b_s^\dagger b_{h1})b_m a_n \ .$$

Applying these recipes and also using the anti-commutation relations to symmetrize the similar terms, we obtain

$$
\begin{aligned}
i\hbar\frac{\partial}{\partial t}b_{h1}a_{e1} &= \varepsilon_{e1}^e b_{h1}a_{e1} - \varepsilon_{h1}^h a_{e1}b_{h1} - \vec{\mu}_{e1h1}\cdot\vec{\mathcal{E}}(t) + \sum_m \vec{\mu}_{e1m}\cdot\vec{\mathcal{E}}(t)b_m^\dagger b_{h1} \\
&+ \sum_n \vec{\mu}_{nh1}\cdot\vec{\mathcal{E}}(t)a_n^\dagger a_{e1} + \sum_{n,m,r} W_{nm}^{re1}a_r^\dagger b_{h1}a_m a_n \\
&- \sum_{n,m,r} W_{nm}^{rh1}b_r^\dagger a_{e1}b_m b_n - \sum_{n,m} W_{nm}^{e1h1}b_m a_n \\
&+ \sum_{n,m,s} W_{nm}^{e1s}b_s^\dagger b_{h1}b_m a_n + \sum_{n,m,r} W_{nm}^{rh1}a_r^\dagger a_{e1}b_m a_n \ .
\end{aligned}
\tag{A.2}
$$

We can now take the expectation values of both sides which will give us the expectation values of four operator terms. By the Hartree-Fock factorization explained in the Chapter 4, we can split the expectation value of four operators products terms in to the products of expectation values of all possible polarizations and/or populations:

$$
\begin{aligned}
\langle a_r^\dagger b_{h1}a_m a_n\rangle &= -\langle a_r^\dagger a_m\rangle\langle b_{h1}a_n\rangle + \langle a_r^\dagger a_n\rangle\langle b_{h1}a_m\rangle \\
&= -p_{rm}p_{nh1} + p_{rn}p_{mh1} \ ,
\end{aligned}
$$

$$
\begin{aligned}
\langle b_r^\dagger a_{e1}b_m b_n\rangle &= \langle b_r^\dagger b_m\rangle\langle b_n a_{e1}\rangle - \langle b_r^\dagger b_n\rangle\langle b_m a_{e1}\rangle \\
&= p_{rm}p_{e1n} - p_{rn}p_{e1m} \ ,
\end{aligned}
$$

$$
\begin{aligned}
\langle b_s^\dagger b_{h1}b_m a_n\rangle &= \langle b_s^\dagger b_{h1}\rangle\langle b_m a_n\rangle - \langle b_s^\dagger b_m\rangle\langle b_{h1}a_n\rangle \\
&= p_{sh1}p_{nm} - p_{sm}p_{nh1} \ ,
\end{aligned}
$$

$$
\begin{aligned}
\langle a_r^\dagger a_{e1}b_m a_n\rangle &= \langle a_r^\dagger a_{e1}\rangle\langle b_m a_n\rangle - \langle a_r^\dagger a_n\rangle\langle b_m a_{e1}\rangle \\
&= p_{re1}p_{nm} - p_{rn}p_{e1m} \ ,
\end{aligned}
$$

where $p_{nm} = b_m a_n$ is the interband polarization, and $p_{nm} = a_n^\dagger a_m$ ($p_{nm} = b_n^\dagger b_m$) gives the electron (hole) intraband polarizations if $n \neq m$ and population distributions if $n = m$.

Inserting these factorization results back to Eq. (A.2) and by specifying general indices with αs for the electron states and βs for the hole states we obtain the expression:

$$
\begin{aligned}
\hbar \frac{\partial}{\partial t} p_{e1h1} &= -i(\varepsilon_{e1}^e + \varepsilon_{h1}^h) p_{e1h1} + i \vec{\mu}_{e1h1} \cdot \vec{\mathcal{E}}(t) - i \sum_\beta \vec{\mu}_{e1\beta} \cdot \vec{\mathcal{E}}(t) p_{\beta h1} \\
&\quad - i \sum_\alpha \vec{\mu}_{\alpha h1} \cdot \vec{\mathcal{E}}(t) p_{\alpha e1} + i \sum_{\alpha,\alpha',\alpha''} W_{\alpha\alpha''}^{\alpha'e1} p_{\alpha'\alpha''} p_{\alpha h1} \\
&\quad - i \sum_{\alpha,\alpha',\alpha''} W_{\alpha''\alpha}^{\alpha'e1} p_{\alpha'\alpha''} p_{\alpha h1} + i \sum_{\beta,\beta',\beta''} W_{\beta\beta'}^{\beta''h1} p_{\beta''\beta'} p_{e1\beta} \\
&\quad - i \sum_{\beta,\beta',\beta''} W_{\beta'\beta}^{\beta''h1} p_{\beta''\beta'} p_{e1\beta} + i \sum_{\alpha,\beta} W_{\alpha\beta}^{e1h1} p_{\alpha\beta} \\
&\quad - i \sum_{\alpha,\beta,\beta'} W_{\alpha\beta'}^{e1\beta} p_{\alpha\beta'} p_{\beta h1} + i \sum_{\alpha,\beta,\beta'} W_{\alpha\beta}^{e1\beta'} p_{\beta'\beta} p_{\alpha h1} \\
&\quad - i \sum_{\alpha,\alpha',\beta} W_{\alpha'\beta}^{\alpha h1} p_{\alpha'\beta} p_{\alpha e1} + i \sum_{\alpha,\alpha',\beta} W_{\alpha\beta}^{\alpha'h1} p_{\alpha'\alpha} p_{e1\beta} \,.
\end{aligned}
$$

Further rearranging similar terms, we get a very general form for the polarization p_{e1h1},

$$
\begin{aligned}
\hbar \frac{\partial}{\partial t} p_{e1h1} &= -i(\varepsilon_{e1}^e + \varepsilon_{h1}^h) p_{e1h1} + i \Big[\vec{\mu}_{e1h1} \cdot \vec{\mathcal{E}}(t) + \sum_{\alpha,\beta} W_{\alpha\beta}^{e1h1} p_{\alpha\beta} \Big] \\
&\quad - i \sum_\beta \Big[\vec{\mu}_{e1\beta} \cdot \vec{\mathcal{E}}(t) + \sum_{\alpha,\beta'} W_{\alpha\beta'}^{e1\beta} p_{\alpha\beta'} \Big] p_{\beta h1} \\
&\quad - i \sum_\alpha \Big[\vec{\mu}_{\alpha h1} \cdot \vec{\mathcal{E}}(t) + \sum_{\alpha',\beta} W_{\alpha'\beta}^{\alpha h1} p_{\alpha'\beta} \Big] p_{\alpha e1} \\
&\quad + i \sum_\alpha \Big[\sum_{\alpha',\alpha''} W_{\alpha\alpha''}^{\alpha'e1} p_{\alpha'\alpha''} - \sum_{\alpha',\alpha''} W_{\alpha''\alpha}^{\alpha'e1} p_{\alpha'\alpha''} + \sum_{\beta,\beta'} W_{\alpha\beta'}^{e1\beta} p_{\beta\beta'} \Big] p_{\alpha h1} \\
&\quad + i \sum_\beta \Big[\sum_{\beta',\beta''} W_{\beta\beta''}^{\beta'h1} p_{\beta'\beta''} - \sum_{\beta',\beta''} W_{\beta''\beta}^{\beta'h1} p_{\beta'\beta''} + \sum_{\alpha,\alpha'} W_{\alpha'\beta}^{\alpha h1} p_{\alpha\alpha'} \Big] p_{e1\beta} \quad \text{(A.3)}
\end{aligned}
$$

Nextly, we derive the equations of motions for the electron populations and intraband electron transitions. Calculation steps are very similar. For the generalization consider the operator, $a_{e1}^\dagger a_{e2}$;

$$
i\hbar \frac{\partial}{\partial t} a_{e1}^\dagger a_{e2} = [a_{e1}^\dagger a_{e2}, \mathcal{H}] \,. \tag{A.4}
$$

when we insert the system Hamiltonian Eq. (4.1) in the right hand side, we need to calculate the following terms,

$$
\begin{aligned}
[a_{e1}^\dagger a_{e2}, a_n^\dagger a_n] &= a_{e1}^\dagger \{a_{e2}, a_n^\dagger\} a_n - a_n^\dagger \{a_{e1}^\dagger, a_n\} a_{e2} \\
&= \delta_{e2n} a_{e1}^\dagger a_n - \delta_{e1n} a_n^\dagger a_{e2},
\end{aligned}
$$

$$
[a_{e1}^\dagger a_{e2}, b_m^\dagger b_m] = 0,
$$

$$
[a_{e1}^\dagger a_{e2}, a_n^\dagger b_m^\dagger] = a_{e1}^\dagger \{a_{e2}, a_n^\dagger\} b_m^\dagger = \delta_{e2n} a_{e1}^\dagger b_m^\dagger,
$$

$$
[a_{e1}^\dagger a_{e2}, b_m a_n] = -b_m \{a_{e1}^\dagger, a_n\} a_{e2} = -\delta_{e1n} b_m a_{e2},
$$

$$
\begin{aligned}
[a_{e1}^\dagger a_{e2}, a_r^\dagger a_s^\dagger a_m a_n] &= [a_{e1}^\dagger a_{e2}, a_r^\dagger a_s^\dagger] a_m a_n + a_r^\dagger a_s^\dagger [a_{e1}^\dagger a_{e2}, a_m a_n] \\
&= a_{e1}^\dagger \{a_{e2}, a_r^\dagger\} a_s^\dagger a_m a_n + a_r^\dagger a_{e1}^\dagger \{a_{e2}, a_s^\dagger\} a_m a_n \\
&\quad - a_r^\dagger a_s^\dagger \{a_{e1}^\dagger, a_m\} a_{e2} a_n^\dagger - a_r^\dagger a_s^\dagger a_m \{a_{e1}^\dagger, a_n\} a_{e2},
\end{aligned}
$$

$$
[a_{e1}^\dagger a_{e2}, b_r^\dagger b_s^\dagger b_m b_n] = 0,
$$

$$
\begin{aligned}
[a_{e1}^\dagger a_{e2}, a_r^\dagger b_s^\dagger b_m a_n] &= [a_{e1}^\dagger a_{e2}, a_r^\dagger b_s^\dagger] b_m a_n + a_r^\dagger b_s^\dagger [a_{e1}^\dagger a_{e2}, b_m a_n] \\
&= a_{e1}^\dagger \{a_{e2}, a_r^\dagger\} b_s^\dagger b_m a_n - a_r^\dagger b_s^\dagger b_m \{a_{e1}^\dagger, a_n\} a_{e2}.
\end{aligned}
$$

We can insert these results back into Eq. (A.4) and summing over corresponding Kronecker δ-functions

$$
\begin{aligned}
i\hbar \frac{\partial}{\partial t} a_{e1}^\dagger a_{e2} &= \varepsilon_{e2}^e a_{e1}^\dagger a_{e2} - \varepsilon_{e1}^e a_{e1}^\dagger a_{e2} - \sum_m (\vec{\mu}_{e2m} a_{e1}^\dagger b_m^\dagger - \vec{\mu}_{me1} b_m a_{e2}) \cdot \vec{\mathcal{E}}(t) \\
&\quad + \frac{1}{2} \sum_{n,m,s} W_{nm}^{e2s} a_{e1}^\dagger a_s^\dagger a_m a_n + \frac{1}{2} \sum_{n,m,r} W_{nm}^{re2} a_r^\dagger a_{e1}^\dagger a_m a_n \\
&\quad - \frac{1}{2} \sum_{n,r,s} W_{ne1}^{rs} a_r^\dagger a_s^\dagger a_{e2} a_n - \frac{1}{2} \sum_{m,r,s} W_{e1m}^{rs} a_r^\dagger a_s^\dagger a_m a_{e2} \\
&\quad - \sum_{n,m,s} W_{nm}^{e2s} a_{e1}^\dagger b_s^\dagger b_m a_n + \sum_{m,r,s} W_{e1m}^{rs} a_r^\dagger b_s^\dagger b_m a_{e2}.
\end{aligned}
$$

As we did in the polarization part playing with indices to collect the similar Coulombic terms we get:

$$
\begin{aligned}
i\hbar\frac{\partial}{\partial t}a_{e1}^{\dagger}a_{e2} &= \varepsilon_{e2}^{e}a_{e1}^{\dagger}a_{e2} - \varepsilon_{e1}^{e}a_{e1}^{\dagger}a_{e2} - \sum_{m}(\vec{\mu}_{e2m}a_{e1}^{\dagger}b_{m}^{\dagger} - \vec{\mu}_{me1}b_{m}a_{e2})\cdot\vec{\mathcal{E}}(t) \\
&+ \sum_{n,m,s}W_{nm}^{e2s}a_{e1}^{\dagger}a_{s}^{\dagger}a_{m}a_{n} - \sum_{m,r,s}W_{e1m}^{rs}a_{r}^{\dagger}a_{s}^{\dagger}a_{m}a_{e2} \\
&- \sum_{n,m,s}W_{nm}^{e2s}a_{e1}^{\dagger}b_{s}^{\dagger}b_{m}a_{n} + \sum_{m,r,s}W_{e1m}^{rs}a_{r}^{\dagger}b_{s}^{\dagger}b_{m}a_{e2}\,.
\end{aligned}
\tag{A.5}
$$

After taking the expectation values of both sides, we can apply the Hartree-Fock factorization such that,

$$
\begin{aligned}
\langle a_{e1}^{\dagger}a_{s}^{\dagger}a_{m}a_{n}\rangle &= -\langle a_{e1}^{\dagger}a_{m}\rangle\langle a_{s}^{\dagger}a_{n}\rangle + \langle a_{e1}^{\dagger}a_{n}\rangle\langle a_{s}^{\dagger}a_{m}\rangle \\
&= -p_{e1m}p_{sn} + p_{e1n}p_{sm}\,,
\end{aligned}
$$

$$
\begin{aligned}
\langle a_{r}^{\dagger}a_{s}^{\dagger}a_{m}a_{e2}\rangle &= -\langle a_{r}^{\dagger}a_{m}\rangle\langle a_{s}^{\dagger}a_{e2}\rangle + \langle a_{r}^{\dagger}a_{e2}\rangle\langle a_{s}^{\dagger}a_{m}\rangle \\
&= -p_{rm}p_{se2} + p_{re2}p_{sm}\,,
\end{aligned}
$$

$$
\begin{aligned}
\langle a_{e1}^{\dagger}b_{s}^{\dagger}b_{m}a_{n}\rangle &= \langle (b_{s}a_{e1})^{\dagger}\rangle\langle b_{m}a_{n}\rangle + \langle a_{e1}^{\dagger}a_{n}\rangle\langle b_{s}^{\dagger}b_{m}\rangle \\
&= p_{e1s}^{*}p_{nm} + p_{e1n}p_{sm}\,,
\end{aligned}
$$

$$
\begin{aligned}
\langle a_{r}^{\dagger}b_{s}^{\dagger}b_{m}a_{e2}\rangle &= \langle (b_{s}a_{r})^{\dagger}\rangle\langle b_{m}a_{e2}\rangle + \langle a_{r}^{\dagger}a_{e2}\rangle\langle b_{s}^{\dagger}b_{m}\rangle \\
&= p_{rs}^{*}p_{e2m} + p_{re2}p_{sm}\,.
\end{aligned}
$$

Inserting these factorized terms into Eq. (A.5), and using again αs for electron states and βs for hole states in order to get out of confusion of indices, we end up with a general equation,

$$
\begin{aligned}
\hbar\frac{\partial}{\partial t}p_{e1e2} &= -i\left(\varepsilon_{e2}^{e} - \varepsilon_{e1}^{e}\right)p_{e1e2} + i\sum_{\beta}(\vec{\mu}_{e2\beta}p_{e1\beta}^{*} - \vec{\mu}_{\beta e1}p_{e2\beta})\cdot\vec{\mathcal{E}}(t) \\
&+ i\sum_{\alpha,\alpha',\alpha''}W_{\alpha''\alpha}^{e2\alpha'}p_{\alpha'\alpha''}p_{e1\alpha} - i\sum_{\alpha,\alpha',\alpha''}W_{\alpha\alpha''}^{e2\alpha'}p_{\alpha'\alpha''}p_{e1\alpha} \\
&- i\sum_{\alpha,\alpha',\alpha''}W_{e1\alpha''}^{\alpha'\alpha}p_{\alpha'\alpha''}p_{\alpha e2} + i\sum_{\alpha,\alpha',\alpha''}W_{e1\alpha''}^{\alpha\alpha'}p_{\alpha'\alpha''}p_{\alpha e2} \\
&+ i\sum_{\alpha,\beta,\beta'}W_{\alpha\beta'}^{e2\beta}p_{\alpha\beta'}p_{e1\beta}^{*} + i\sum_{\alpha,\beta,\beta'}W_{\alpha\beta'}^{e2\beta}p_{\beta\beta'}p_{e1\alpha} \\
&- i\sum_{\alpha,\beta,\beta'}W_{e1\beta}^{\alpha\beta'}p_{\alpha\beta'}^{*}p_{e2\beta} - i\sum_{\alpha,\beta,\beta'}W_{e1\beta'}^{\alpha\beta}p_{\beta\beta'}p_{\alpha e2}\,.
\end{aligned}
$$

In order to obtain a similar expression to the interband polarization expression Eq. (A.3), we rearrange the terms and obtain a general equation for both electron populations and electron intraband polarizations,

$$
\begin{aligned}
\hbar \frac{\partial}{\partial t} p_{e1e2} &= -i \left(\varepsilon_{e2}^e - \varepsilon_{e1}^e \right) p_{e1e2} + i \sum_\beta \left[\vec{\mu}_{e2\beta} \cdot \vec{\mathcal{E}}(t) + \sum_{\alpha,\beta'} W_{\alpha\beta'}^{e2\beta} p_{\alpha\beta'} \right] p_{e1\beta}^* \\
&\quad - i \sum_\beta \left[\vec{\mu}_{\beta e1} \cdot \vec{\mathcal{E}}(t) + \sum_{\alpha,\beta'} W_{e1\beta}^{\alpha\beta'} p_{\alpha\beta'}^* \right] p_{e2\beta} \\
&\quad + i \sum_\alpha \left[\sum_{\alpha',\alpha''} W_{\alpha''\alpha}^{e2\alpha'} p_{\alpha'\alpha''} - \sum_{\alpha',\alpha''} W_{\alpha\alpha''}^{e2\alpha'} p_{\alpha'\alpha''} + \sum_{\beta,\beta'} W_{\alpha\beta'}^{e2\beta} p_{\beta\beta'} \right] p_{e1\alpha} \\
&\quad - i \sum_\alpha \left[\sum_{\alpha',\alpha''} W_{e1\alpha'}^{\alpha''\alpha} p_{\alpha''\alpha'} - \sum_{\alpha',\alpha''} W_{e1\alpha'}^{\alpha\alpha''} p_{\alpha''\alpha'} + \sum_{\beta,\beta'} W_{e1\beta}^{\alpha\beta'} p_{\beta'\beta} \right] p_{\alpha e2} \quad \text{(A.6)}
\end{aligned}
$$

Derivation of such a general equation makes the derivations shorter. It is because if we let $e1 = e2$, then Eq. (A.6) will give the equation of motion for the electron population of state $|e1\rangle$. Otherwise, for $e1 \neq e2$, it will reduce to the equation of motion for the intraband polarization $p_{e1e2} = \langle a_{e1}^\dagger a_{e2} \rangle$ between the states $|e1\rangle$ and $|e2\rangle$. However, for the sake of computational implementation we use the same expression for both populations and polarizations. Otherwise, we should write two general equations; one for electron populations n_{e_i} and one for electron intraband polarizations $p_{e_i e_j}$. In total we should have 5 general equation of motions as $p_{e_i h_j}$, n_{e_i}, $p_{e_i e_j}$, n_{h_i}, and $p_{h_i h_j}$. Instead of that we keep 3 equations of motions $p_{e_i h_j}$, $p_{e_i e_j}$, and $p_{h_i h_j}$ and just keep in mind that when $i = j$ the last two expressions give the electron and hole populations, respectively.

Finally we derive the equations of motions for the hole populations and intraband hole transitions. For the generalization we consider the operator, $b_{h1}^\dagger b_{h2}$;

$$
i\hbar \frac{\partial}{\partial t} b_{h1}^\dagger b_{h2} = [b_{h1}^\dagger b_{h2}, \mathcal{H}] , \quad \text{(A.7)}
$$

The terms in the right hand side are calculated using Eqs. (4.18-4.20), we get:

$$
[b_{h1}^\dagger b_{h2}, a_n^\dagger a_n] = 0 ,
$$

$$
\begin{aligned}
[b_{h1}^\dagger b_{h2}, b_m^\dagger b_m] &= b_{h1}^\dagger \{b_{h2}, b_m^\dagger\} b_m - b_m^\dagger \{b_{h1}^\dagger, b_m\} b_{h2} \\
&= \delta_{h2m} b_{h1}^\dagger b_m - \delta_{h1m} b_m^\dagger b_{h2} ,
\end{aligned}
$$

$$[b_{h1}^\dagger b_{h2}, a_n^\dagger b_m^\dagger] = a_n^\dagger b_{h1}^\dagger \{b_{h2}, b_m^\dagger\} = \delta_{h2m} a_n^\dagger b_{h1}^\dagger \,,$$

$$[b_{h1}^\dagger b_{h2}, b_m a_n] = -\{b_{h1}^\dagger, b_m\} b_{h2} a_n = -\delta_{h1m} b_{h2} a_n \,,$$

$$[b_{h1}^\dagger b_{h2}, a_r^\dagger a_s^\dagger a_m a_n] = [b_{h1}^\dagger b_{h2}, a_r^\dagger a_s^\dagger] a_m a_n + a_r^\dagger a_s^\dagger [b_{h1}^\dagger b_{h2}, a_m a_n] = 0 \,,$$

$$\begin{aligned}
[b_{h1}^\dagger b_{h2}, b_r^\dagger b_s^\dagger b_m b_n] &= [b_{h1}^\dagger b_{h2}, b_r^\dagger b_s^\dagger] b_m b_n + b_r^\dagger b_s^\dagger [b_{h1}^\dagger b_{h2}, b_m b_n] \\
&= b_{h1}^\dagger \{b_{h2}, b_r^\dagger\} b_s^\dagger b_m b_n + b_r^\dagger b_{h1}^\dagger \{b_{h2}, b_s^\dagger\} b_m b_n - b_r^\dagger b_s^\dagger \{b_{h1}^\dagger, b_m\} b_{h2} b_m \\
&\quad - b_r^\dagger b_s^\dagger b_m \{b_{h1}^\dagger, b_n\} b_{h2} \,,
\end{aligned}$$

$$\begin{aligned}
[b_{h1}^\dagger b_{h2}, a_r^\dagger b_s^\dagger b_m a_n] &= [b_{h1}^\dagger b_{h2}, a_r^\dagger b_s^\dagger] b_m a_n + a_r^\dagger b_s^\dagger [b_{h1}^\dagger b_{h2}, b_m a_n] \\
&= a_r^\dagger b_{h1}^\dagger \{b_{h2}, b_s^\dagger\} b_m a_n - a_r^\dagger b_s^\dagger \{b_{h1}^\dagger, b_m\} b_{h2} a_n \,.
\end{aligned}$$

Now we insert all these commutation terms back into Eq. (A.7),

$$\begin{aligned}
i\hbar \frac{\partial}{\partial t} b_{h1}^\dagger b_{h2} &= \varepsilon_{h2}^h b_{h1}^\dagger b_{h2} - \varepsilon_{h1}^h b_{h1}^\dagger b_{h2} - \sum_n (\vec{\mu}_{nh2} a_n^\dagger b_{h1}^\dagger - \vec{\mu}_{h1n} b_{h2} a_n) \cdot \vec{\mathcal{E}}(t) \\
&\quad + \frac{1}{2} \sum_{n,m,s} W_{nm}^{h2s} b_{h1}^\dagger b_s^\dagger b_m b_n + \frac{1}{2} \sum_{n,m,r} W_{nm}^{rh2} b_r^\dagger b_{h1}^\dagger b_m b_n \\
&\quad - \frac{1}{2} \sum_{n,r,s} W_{nh1}^{rs} b_r^\dagger b_s^\dagger b_{h2} b_m - \frac{1}{2} \sum_{m,r,s} W_{h1m}^{rs} b_r^\dagger b_s^\dagger b_m b_{h2} \\
&\quad - \sum_{n,m,r} W_{nm}^{rh2} a_r^\dagger b_{h1}^\dagger b_m a_n + \sum_{n,r,s} W_{nh1}^{rs} a_r^\dagger b_s^\dagger b_{h2} a_n \,.
\end{aligned}$$

As it was in the above discussion, here again the first and second Coulomb interaction terms are identical after some arrangement. Similarly the third and fourth ones are same. Summing over corresponding Kronecker delta indices we obtain,

$$\begin{aligned}
i\hbar \frac{\partial}{\partial t} b_{h1}^\dagger b_{h2} &= \varepsilon_{h2}^h b_{h1}^\dagger b_{h2} - \varepsilon_{h1}^h b_{h1}^\dagger b_{h2} - \sum_n (\vec{\mu}_{nh2} a_n^\dagger b_{h1}^\dagger - \vec{\mu}_{h1n} b_{h2} a_n) \cdot \vec{\mathcal{E}}(t) \\
&\quad + \sum_{n,m,s} W_{nm}^{h2s} b_{h1}^\dagger b_s^\dagger b_m b_n - \sum_{n,r,s} W_{nh1}^{rs} b_r^\dagger b_s^\dagger b_{h2} b_m \\
&\quad - \sum_{n,m,r} W_{nm}^{rh2} a_r^\dagger b_{h1}^\dagger b_m a_n + \sum_{n,r,s} W_{nh1}^{rs} a_r^\dagger b_s^\dagger b_{h2} a_n \,. \qquad \text{(A.8)}
\end{aligned}$$

After taking the expectation values of both sides, we can apply the factorization to four-operator terms,

$$\langle b_{h1}^\dagger b_s^\dagger b_m b_n \rangle = -\langle b_{h1}^\dagger b_m \rangle \langle b_s^\dagger b_n \rangle + \langle b_{h1}^\dagger b_n \rangle \langle b_s^\dagger b_m \rangle$$
$$= -p_{h1m}p_{sn} + p_{h1n}p_{sm},$$

$$\langle b_r^\dagger b_s^\dagger b_{h2} b_n \rangle = -\langle b_r^\dagger b_{h2} \rangle \langle b_s^\dagger b_n \rangle + \langle b_r^\dagger b_n \rangle \langle b_s^\dagger b_{h2} \rangle$$
$$= -p_{rh2}p_{sn} + p_{rn}p_{sh2},$$

$$\langle a_r^\dagger b_{h1}^\dagger b_m a_n \rangle = \langle a_r^\dagger a_n \rangle \langle b_{h1}^\dagger b_m \rangle + \langle (b_{h1}a_r)^\dagger \rangle \langle b_m a_n \rangle$$
$$= p_{rn}p_{h1m} + p_{rh1}^* p_{nm},$$

$$\langle a_r^\dagger b_s^\dagger b_{h2} a_n \rangle = \langle (b_s a_r)^\dagger \rangle \langle b_{h2} a_n \rangle + \langle a_r^\dagger a_n \rangle \langle b_s^\dagger b_{h2} \rangle$$
$$= p_{rs}^* p_{nh2} + p_{rn}p_{sh2}.$$

Inserting these factorized expression into Eq. (A.8), and switching to αs and βs for state indices, we obtain a very general relation

$$\hbar \frac{\partial}{\partial t} p_{h1h2} = -i \left(\varepsilon_{h2}^h - \varepsilon_{h1}^h \right) p_{h1h2} + i \sum_\alpha \left(\vec{\mu}_{\alpha h2} p_{\alpha h1}^* - \vec{\mu}_{h1\alpha} p_{\alpha h2} \right) \cdot \vec{\mathcal{E}}(t)$$
$$+ i \sum_{\beta,\beta',\beta''} W_{\beta\beta'}^{h2\beta''} p_{h1\beta'} p_{\beta''\beta} - i \sum_{\beta,\beta',\beta''} W_{\beta\beta'}^{h2\beta''} p_{h1\beta} p_{\beta''\beta'}$$
$$- i \sum_{\beta,\beta',\beta''} W_{\beta h1}^{\beta'\beta''} p_{\beta'h2} p_{\beta''\beta} + i \sum_{\beta,\beta',\beta''} W_{\beta h1}^{\beta'\beta''} p_{\beta'\beta} p_{\beta''h2}$$
$$+ i \sum_{\alpha,\alpha',\beta} W_{\alpha\beta}^{\alpha'h2} p_{\alpha'\alpha} p_{h1\beta} + i \sum_{\alpha,\alpha',\beta} W_{\alpha\beta}^{\alpha'h2} p_{\alpha'h1}^* p_{\alpha\beta}$$
$$- i \sum_{\alpha,\alpha',\beta} W_{\alpha h1}^{\alpha'\beta} p_{\alpha'\beta}^* p_{\alpha h2} - i \sum_{\alpha,\alpha',\beta} W_{\alpha h1}^{\alpha'\beta} p_{\alpha'\alpha} p_{\beta h2}.$$

Further arranging the terms we obtain the equation of motion for the hole populations and intraband polarizations:

$$\hbar \frac{\partial}{\partial t} p_{h1h2} = -i \left(\varepsilon_{h2}^h - \varepsilon_{h1}^h \right) p_{h1h2} + i \sum_\alpha \left[\vec{\mu}_{\alpha h2} \cdot \vec{\mathcal{E}}(t) + \sum_{\alpha',\beta} W_{\alpha'\beta}^{\alpha h2} p_{\alpha'\beta} \right] p_{\alpha h1}^*$$
$$- i \sum_\alpha \left[\vec{\mu}_{h1\alpha} \cdot \vec{\mathcal{E}}(t) + \sum_{\alpha',\beta} W_{\alpha h1}^{\alpha'\beta} p_{\alpha'\beta}^* \right] p_{\alpha h2}$$
$$+ i \sum_\beta \left[\sum_{\beta',\beta''} W_{\beta''\beta}^{h2\beta'} p_{\beta'\beta''} - \sum_{\beta',\beta''} W_{\beta\beta''}^{h2\beta'} p_{\beta'\beta''} + \sum_{\alpha,\alpha'} W_{\alpha'\beta}^{\alpha h2} p_{\alpha\alpha'} \right] p_{h1\beta}$$
$$- i \sum_\beta \left[\sum_{\beta',\beta''} W_{\beta'h1}^{\beta\beta''} p_{\beta''\beta'} - \sum_{\beta',\beta''} W_{\beta'h1}^{\beta''\beta} p_{\beta''\beta'} + \sum_{\alpha,\alpha'} W_{\alpha h1}^{\alpha'\beta} p_{\alpha'\alpha} \right] p_{\beta h2}. \text{ (A.9)}$$

Now one can specialize this equation. For $h1 = h2$ the expectation value $\langle b_{h1}^{\dagger} b_{h1} \rangle$ will yield the hole population n_{h1} for the state $|h1\rangle$. Instead of that, if we state that $h1 \neq h2$, the expectation value $\langle b_{h1}^{\dagger} b_{h2} \rangle$ gives the intraband transition p_{h1h2} between the hole states $|h1\rangle$ and $|h2\rangle$. However, as we mentioned in the electron part, we keep the expression in general form for the sake of computational simplicity and bookkeeping.